

17

# A TRIDENT SCHOLAR PROJECT REPORT

AD-A171 743

NO.  
140

ENVIRONMENTAL EFFECTS ON IMPACT DAMAGE  
TOLERANCE OF HYBRID COMPOSITE MATERIAL.



DTIC  
ELECTE  
SEP 09 1986  
S D

UNITED STATES NAVAL ACADEMY  
ANNAPOLIS, MARYLAND  
1986

This document has been approved for public  
release and sale; its distribution is unlimited.

DTIC FILE COPY

UNCLASSIFIED

SECURITY CLASSIFICATION OF THIS PAGE (When Data Entered)

REPORT DOCUMENTATION PAGE		READ INSTRUCTIONS BEFORE COMPLETING FORM
1. REPORT NUMBER U.S.N.A. - TSPR; no. 140 (1986)	2. GOVT ACCESSION NO. <b>AD-A171743</b>	3. RECIPIENT'S CATALOG NUMBER
4. TITLE (and Subtitle) ENVIRONMENTAL EFFECTS ON IMPACT DAMAGE TOLERANCE OF HYBRID COMPOSITE MATERIAL.	5. TYPE OF REPORT & PERIOD COVERED Final: 1985/1986	
	6. PERFORMING ORG. REPORT NUMBER	
7. AUTHOR(s) Wood, Lawrence E.	8. CONTRACT OR GRANT NUMBER(s)	
9. PERFORMING ORGANIZATION NAME AND ADDRESS United States Naval Academy, Annapolis.	10. PROGRAM ELEMENT, PROJECT, TASK AREA & WORK UNIT NUMBERS	
11. CONTROLLING OFFICE NAME AND ADDRESS United States Naval Academy, Annapolis.	12. REPORT DATE 28 May 1986	
	13. NUMBER OF PAGES 52	
14. MONITORING AGENCY NAME & ADDRESS (if different from Controlling Office)	15. SECURITY CLASS. (of this report)	
	15a. DECLASSIFICATION/DOWNGRADING SCHEDULE	
16. DISTRIBUTION STATEMENT (of this Report)  This document has been approved for public release; its distribution is UNLIMITED.		
17. DISTRIBUTION STATEMENT (of the abstract entered in Block 20, if different from Report)  This document has been approved for public release; its distribution is UNLIMITED.		
18. SUPPLEMENTARY NOTES  Accepted by the U.S. Trident Scholar Committee.		
19. KEY WORDS (Continue on reverse side if necessary and identify by block number)  Composite materials Graphite fibers		
20. ABSTRACT (Continue on reverse side if necessary and identify by block number)  ▶The behavior of an intraply hybrid composite material of polyethylene and graphite fibers in an epoxy matrix under the effects of environmental conditioning, impact damage, and fatigue loading was investigated. Although the ultimate tensile strength of the hybrid material was found to be lower than that of graphite material alone, the specific strengths of the materials were comparable. Dye-penetrant enhanced X-ray radiography and edge replication were (OVER) -		

DD FORM 1473  
1 JAN 73EDITION OF 1 NOV 65 IS OBSOLETE  
S. N. 0102-LF-014-6601

UNCLASSIFIED

SECURITY CLASSIFICATION OF THIS PAGE (When Data Entered)

UNCLASSIFIED

SECURITY CLASSIFICATION OF THIS PAGE (When Data Entered)

used to evaluate the damage growth of the test material. Impact damage evaluations showed the initial crack tolerance of the hybrid materials was better than that of conventional graphite. Specimens of both materials were soaked in standard ocean water and their moisture absorption observed. The moisture absorption percentages for the hybrid and graphite materials were 2.91 percent and 1.47 percent by weight respectively. Both dry and wet hybrid material was subjected to impact and fatigue loading. During fatigue loading the hybrid material exhibited viscoelastic behavior characterized by a non-linear loading curve. The wet hybrid material experienced both a sharper reduction in stiffness, and a greater increase in damage area than the dry material.

S/N 0102-LF-014-6601

UNCLASSIFIED

SECURITY CLASSIFICATION OF THIS PAGE(When Data Entered)

U.S.N.A. - Trident Scholar project report; no. 140 (1986)

Environmental Effects on Impact Damage Tolerance  
of Hybrid Composite Material

A Trident Scholar Project Report

by

Midshipman First Class Lawrence E. Wood  
Class of 1986  
U.S. Naval Academy  
Annapolis, Maryland 21403

*Russell D. Jamison*

Asst Prof R. D. Jamison - M.E. Dept  
Advisor

Accepted for Trident Scholar Committee

*Carl Schieler*

Chairman

*28 Mar 1986*

Date



Accession For	
NTIS CRA&I	<input checked="" type="checkbox"/>
DTIC TAB	<input type="checkbox"/>
Unannounced	<input type="checkbox"/>
Justification	
By	
Distribution/	
Availability Codes	
Dist	Avail and/or Special
A-1	

# Environmental Effects on Impact Damage Tolerance of Hybrid Composite Material

*Lawrence E. Wood*

United States Naval Academy

## *ABSTRACT*

The behavior of an intraply hybrid composite material of polyethylene and graphite fibers in an epoxy matrix under the effects of environmental conditioning, impact damage, and fatigue loading was investigated. Although the ultimate tensile strength of the hybrid material was found to be lower than that of graphite material alone, the specific strengths of the materials were comparable. Dye-penetrant enhanced X-ray radiography and edge replication were used to evaluate the damage growth of the test material. Impact damage evaluations showed the initial crack tolerance of the hybrid material was better than that of conventional graphite. Specimens of both materials were soaked in standard ocean water and their moisture absorption observed. The moisture absorption percentages for the hybrid and graphite materials were 2.91% and 1.47% by weight respectively. Both dry and wet hybrid material was subjected to impact and fatigue loading. During fatigue loading the hybrid material exhibited viscoelastic behavior characterized by a non-linear loading curve. The wet hybrid material experienced both a sharper reduction in stiffness, and a greater increase in damage area than the dry material.

**Table of Contents**

List of Illustrations/Tables	3
Introduction	4
Review of Literature	6
Experimental Program	
Test Material and Fabrication	9
Specimen Preparation	10
Static Testing	11
Impact Damage	12
Environmental Conditioning	13
Fatigue Testing	1
Nondestructive Evaluation	
1. Edge Replication	17
2. X-ray Radiography	18
3. Ultrasonic C-scan	19
Discussion of Results	20
Conclusions	26
Illustrations	28
Tables	48
Acknowledgements	50
References	51
Appendix A	52

**List of Illustrations**

1.	Resin Properties	28
2.	Plain Weave	29
3.	Hybrid Weave Pattern	30
4.	Material Cure Cycle	31
5.	Fatigue Testing Arrangement	32
6.	Drop Tower Arrangement	33
7.	Constraint Fixture	34
8.	Data Acquisition System	35
9.	Typical Stiffness Reduction Curve	36
10.	Dye Penetrant Infiltration Arrangement	37
11.	Hysteresis Curves - Dry Material	38
12.	Hysteresis Curves - Wet Material	39
13.	Stiffness Reduction Curve - Dry Material	40
14.	Stiffness Reduction Curve - Wet Material	41
15.	Damage Growth in Dry Material	42
16.	Damage Growth in Wet Material	43
17.	Summary of Damage Growth in Dry Material	44
18.	Summary of Damage Growth in Wet Material	45
19.	Typical Edge Replicas	46
20.	Fatigue Failure Example	47

**List of Tables**

1.	Static Testing Summary	48
2.	Moisture Absorption Results	49

## Introduction

Perhaps one of the most fundamental inquiries in Naval research today is the question of what the future holds with respect to material technology. What developments in current research made in this area will improve the ability of the Navy to perform its mission in the future? In recent years, great strides have been made in composite material research and development which may significantly alter the composition of the hardware of the future Navy. Composite materials are already in use in some marine and aviation applications today. The Navy's AV-8B and V-22 aircraft, for example, utilize advanced composite materials in primary structures. Yet there still exist opportunities for improvement in the characterization of the behavior of these materials in order for their full potential to be realized.

Composite materials are those in which two or more constituents are combined on a *macroscopic* level. Composites can exhibit the best qualities of their constituents and often some qualities that neither constituent possesses individually. Composite materials range from the simple straw-mud bricks used by the ancient Israelites to the advanced fiber-reinforced composites in use today. An important class of composites consists of uniaxial or woven organic or inorganic fibers bound together by an epoxy matrix to form a ply or lamina. When stacked in varying orientations, these plies form a lightweight material of considerable specific strength and specific stiffness† uniquely suited for many structural applications.

Growing future use of composite materials in naval applications is inevitable in the opinion of many [1-6]. It is important therefore that candidate composite materials for Navy applications be thoroughly characterized and their potential for reliable, predictable, in-service behavior be assessed. One relatively new area of investigation in fibrous composite development involves hybrid composite materials. Hybrid composites extend

---

† A specific property of a material is defined as that property divided by the material's density. Comparison of specific properties provides a rational basis for material selection.

fiber composites beyond the traditional one fiber, one matrix concept by introducing multiple types of fibers into a single matrix. Hybrid composites were developed to meet diverse and competing design requirements in a more cost-effective way than either advanced or conventional composites [1]. Before optimum structural utilization of these new materials can be fully realized, it is important that their properties be determined under both laboratory conditions and anticipated service conditions, the latter being potentially far more aggressive.

A widely used composite material, graphite/epoxy, has proven itself in many aviation structural applications. However, it was conceivable that the brittle characteristics of this material might be compensated by the addition of the more ductile polyethylene fibers. The current experimental program was aimed at determining the static mechanical properties (modulus and ultimate tensile strength) of a candidate hybrid composite material, and investigating its behavior under conditions simulating a likely service environment. The material investigated was an intraply hybrid composite of graphite and polyethylene fibers suspended in an Epon 826 epoxy resin matrix.

Composite material aviation structures will experience cyclic loading. As a result, impact damage growth and its possible interaction with high moisture content become factors which must be investigated. This project focused primarily on three goals: static testing, which provided fundamental structural characteristics for fatigue testing; evaluation of damage growth due to axial fatigue loading; and evaluation of damage growth tolerance reduction due to high moisture content.

This report includes a review of the literature available on the subjects of hybrid composite behavior, impact damage tolerance of composites, and methods of Nondestructive Evaluation (NDE) utilized. The subsequent section documents the rationale and structure of the investigation. Finally, a discussion of results compares the behavior of the hybrid composite with that of conventional graphite, investigating both the failure mechanisms and damage tolerance.

## Review of Literature

In recent years hybrid composite material research has become an increasingly active field. As a result, the amount of literature in this area has increased accordingly. There also exists a large number of articles related to experimental methods, environmental conditioning, and analytical approaches to laminate analysis, all of which were subjects encountered in this study.

Two properties of hybrid composite materials which make them attractive to designers for potential use in structural applications are high specific strength and impact damage resistance. In weight-sensitive applications, such as aircraft components, it is especially important that structures be able to support a desired load, yet at the same time, not reduce available power by adding significantly to the aircraft's weight. In dealing with conventional graphite composites used in many load-bearing applications on an aircraft, the greatest threat of failure is not the result of a potential static overload. Rather, the greatest threat of failure at this point in composite utilization stems from the failure associated with impact damage [2]. The brittle nature of the individual graphite fiber contributes to the brittle behavior of the laminate. It is then the intention of the hybrid composite material fabricator to toughen these laminates by the addition of a material possessing a more ductile individual behavior. As with steel and other metals, with toughness comes sacrifice of strength and modulus of elasticity.

In designing a hybrid composite for toughness, it is then necessary to understand the discrete modes by which composites in general fail. Jamison, Shulte, Reifsnider, and Stinchcomb [3] discussed the fiber fracture mechanisms in 0-degree plies in conventional graphite composites subjected to tension-tension fatigue. They concluded that ultimate failure results from a fiber damage condition initiating in the plies. Hence, the ply becomes a fundamental component in the understanding of composite material failure. In the opinion of many [3,4], the ply becomes "the center of activity" for severe damage growth in the composite. Consequently, it was the intention of this program to investigate

a hybrid composite material in which the individual ply was toughened by intraply\* hybridization.

Although the concept of hybridization was born soon after graphite fiber composites began to be used, research in this area has been slow. Chamis and Lark [1] have presented a *state-of-the-art* survey of hybrid composite materials summarizing the design, application, and fabrication of such materials. They pointed out several areas in which further research is needed including temperature and moisture effects, thermal properties, nonlinear laminate theory for hybrids, and theoretical description of fatigue.

Jones [5] discussed the basic principles of composite material behavior, and pointed out that most composite material properties can be theoretically obtained by accounting for the laminate composition and the individual properties of the constituents. However he did state that restrictions do exist which prevent the accurate attainment of the micromechanical behavior of the composite; the primary restriction being the need for laminar linear elastic behavior.

Adams, Zimmerman, and Chang [6] performed mechanical property measurements on the polyethylene fiber, designated A-900, which was developed by Allied Corporation for potential use in polymer-matrix composites. Their studies indicated that while axial compressive, transverse tensile, and shear properties are low, the axial tensile and impact properties are high, making it an attractive candidate for hybridization with graphite. Also in its favor is its low density which is roughly half that of graphite. Conversely, the study showed that the A-900 fiber did not maintain its properties at temperatures above 250 °F (121 °C). The tensile strength of the polyethylene fiber at 250 °F was slightly more than half the room temperature value. They also recognized that the fiber-matrix interface bond strength was deficient and a shortcoming in comparison to other fiber systems.

---

\* An intraply hybrid is a hybrid in which the individual ply contains more than one type of fiber

Articles investigating conventional graphite composite material properties provided information regarding damage mechanisms and test methods to be used. Jamison et al [3] and Jamison [4], investigating failure mechanisms in graphite laminates, spoke of damage conditions in a composite material in terms of discrete, identifiable damage in the microstructure constituents: fiber, matrix, and fiber-matrix interfaces in each lamina and of the interface between the laminae. He agreed with several researchers that fatigue damage consists of various combinations of matrix cracking, fiber-matrix debonding, delamination, void growth, and local fiber breakage. He recognized that there are factors which affect a material's tolerance to such defects. In his studies, he used dye penetrant enhanced X-ray radiography, edge replication, and other NDE techniques in damage assessment. X-ray radiography was also used by Eaton [7] in his study of ballistic damage of graphite/epoxy plates.

Several investigators have studied the impact damage tolerance of composite materials. Altman and Olsen [8] found that the most frequent damage sustained by horizontally placed aircraft composite components was the result of tool impact. For the purposes of establishing typical indenter geometry and reasonable impact energy levels, impact testing was done in the laboratory. They discovered that energy levels of two to six foot-pounds resulted in defects of similar size and damage characteristics. Ramkumar [9] in his investigation used the dropped ball impact method to initiate the damage in the test material, and found that in order to obtain a consistent area of initial damage from specimen to specimen a constraint was necessary. He used a cylindrical metal ring beneath the intended impact area to constrain the initial damage.

Moisture absorption studies in graphite/epoxy laminates have been undertaken by a number of investigators [9,10,11,12,13,14]. Hancox [12] studied the environmental response of hybrid composites of graphite, Kevlar, and glass fibers in a standard anhydride epoxide resin. The fibers were mixed in various combinations and subjected to varying environmental conditions. His studies concluded that soaking in water caused a

substantial reduction in modulus of all Kevlar fiber/resin combinations, and that the effects of moisture content were significant and irreversible. Other results showed that conventional graphite composites normally absorb 1.2-1.5% moisture by weight in a 60 day period under varying temperatures [8,10,11]. It was found that the matrix-dominated properties were more apt to be affected by the presence of moisture than the fiber-dominated properties [11]. Carswell [13] investigated hysteresis and environmental effects on fatigue of graphite composite materials.

Improvements in composite materials in naval applications were also discussed. Fuss [2] explained the complexity of composite material repair on aircraft. He also stated the need for more temperature resistant composites for use in the vicinity of jet exhausts.

#### **Test Material and Fabrication**

The test material in this study was an intraply hybrid composite consisting of woven polyethylene and graphite fibers. This material was supplied by Allied Corporation and fabricated into laminates by Hexel Corporation. The woven plies were suspended in an epoxy formulation manufactured by Hexel. This resin, designated F155, is a toughness-modified, low-temperature cure Epon-826† epoxy. Figure 1 contains the properties of the resin. The T300 graphite fibers were supplied by Hexel. The remaining fibers in the hybrid composite material were A-900 commercial polyethylene fibers manufactured by Allied. The fibers were woven into plies using a plain weave (Figure 2). The plies were designed with the intention of obtaining a 2:1 ratio of graphite/A-900 fibers. It was thought that a larger percentage of polyethylene in the ply would have resulted in a material whose mechanical behavior was undesirable due to the domination of the polyethylene properties. In order to achieve these percentages in the individual ply it was necessary to weave two graphite tows\* for every tow of polyethylene resulting in a weave pattern as shown in Figure 3.

† Epon-826 is a commercial industry standard

\* A tow is bundle of fibers

After weaving, the plies were then subjected to prepregging, the process by which the matrix is added. The prepregged plies were then fabricated into laminates using a conventional autoclave/vacuum bag bleed system. Figure 4 presents the procedure followed in this curing process. Graphite/epoxy plates of the same weave pattern were also fabricated using the same technique.

After fabrication each panel was measured and given a letter designation. The measured panel thicknesses as received were:

Panel D	(GR/E)	.127 in. (3.22 mm)
Panel G	(GR/E)	.135 in. (3.43 mm)
Panel E	(HYBRID)	.138 in. (3.51 mm)
Panel H	(HYBRID)	.140 in. (3.56 mm)
Panel M	(HYBRID)	.138 in. (3.51 mm)

Although poor adhesion between the polyethylene fiber and resin had been noted [3], it was decided to use commercially available techniques to fabricate the hybrid test material realizing that improvements in this area might be forthcoming.

### Specimen Preparation

The composite test panels were machined into specimens in accordance with the following instructions:

- sawed edges to be as smooth and free of scratches, chips, and loose surface fibers as possible.
- specimens to be cut from the center of each panel discarding at least 0.75 in. (19 mm) from each edge.
- each specimen to be  $8.0 \pm 0.1$  in ( $203 \pm 2.5$  mm) by  $1.75 \pm 0.005$  in. ( $44 \pm 0.127$  mm)

Problems were encountered adhering to these specifications due to the fraying characteristic of the polyethylene fiber. After investigating several alternative techniques, it was determined that a high speed grinder used with a coarse wheel and flooding coolant provided satisfactory sawed-edges.

The ends (approximately 1 3/4 in. (44 mm)) were coated with a thin layer of MS 907 epoxy manufactured by Miller-Stephenson Chemical Company. This coating served to consolidate the surface fibers in the 0 degree direction and provide a more uniform gripping surface for tensile loading. Emery cloth (320 grit) was interposed between the machine grips and the specimens during fatigue loading to improve the gripping efficiency. The epoxy layer served to insulate the specimen from wear induced by the fatigue loading. This preparation arrangement is shown schematically in Figure 5.

The edges of all specimens to be used in fatigue testing were polished using grit paper of successively finer abrasives. This polishing was necessary for edge replication. Edge replication is discussed in detail in a subsequent section of this report.

Each specimen was assigned a code number consisting of the panel letter from which it came and its number within that panel. The figure below depicts how each panel was numbered.

1	2	3	4	5	6	7	8
16	15	14	13	12	11	10	9

This numbering system was used track possible manufacturing flaws which might affect adjoining specimens.

### Static Testing

All static tests were completed on a 60,000 lb. (272.7 kN) capacity Tinius-Olsen Southwark Emery Compression-Tension testing machine. The specimens were secured by mechanical Instron grips having 2 in (50 mm) wide wedges.

Static testing was performed to determine the ultimate tensile strength, UTS, of both graphite/epoxy and the hybrid composite material. These tests were conducted with the testing machine in the displacement-controlled mode using a constant crosshead speed of 0.075 in./min. (2 mm/min.). Six specimens of each material were tested. Stress-strain curves were obtained for each specimen before each was loaded to failure. Strain was measured by means of an extensometer attached to one side of the specimen. The extensometer gage length for these tests was nominally 1 in. (25 mm), and attachment was made to the center portion of the specimen. The extensometer knife edges were seated in narrow, V-shaped channels machined into brass tabs. These tabs, measuring nominally 1/2 in. (13 mm) by 1/4 in. (6 mm) by 1/8 in. (3.2 mm), were in turn bonded to the specimen using RTV silicone rubber cement manufactured by the 3-M Company. Figure 5 shows the placement of these tabs. A summary of the static testing results is presented in Table 1.

### **Impact Damage**

Approximately 75% of the remaining test specimens were subjected to low velocity impact damage prior to fatigue testing. These specimens were damaged utilizing a drop tower located in the Advanced Composite Material Lab, David Taylor Naval Ship Research and Development Center. The drop tower, having a variable-height magnetizing head and steel balls of differing weight, was used to subject each specimen to 120 lbs ( 13.85 N-m). The 2 in. (51.2 mm) diameter ball used weighed 1.18 lb. (0.534 Kg) and was dropped from a height of 102 in. (2.59 m). Figure 6 shows this arrangement. Ramkumar [9] noted that in order to obtain consistent initial damage throughout the specimens, containment of the damage to a constant area was necessary.

It was recognized that initial impact could be accomplished several ways. One method involved impacting the 18" x 18" panel as received. Specimens would then be cut from the panel centering the impact area in each. This method would have resulted in varied clamping constraints, i. e. specimens near the edge of the plate would have been

constrained differently than those nearer to the plate center. These varying constraints would have created inconsistent initial damage. The method chosen instead involved impacting the individual specimens using the "clamped-clamped" constraint. The "clamped-clamped" constraint allowed minimal deflection of the specimen during impact by constraining all four edges. The fixture shown in Figure 7 was used to constrain each edge of the specimen during impact. The constant area containment was accomplished by placing a one inch outer diameter aluminum pipe directly under the impact location of each specimen. The impact damage zone was confirmed by radiography to be confined to a one inch diameter circle equidistant from the edges and centered on the point of impact.

#### **Environmental Conditioning**

American Society of Testing and Materials (ASTM) Standard Substitute Ocean Water was used to environmentally condition the test specimens [15]. Appendix A details the constituents of this solution. One-half of the impacted specimens were totally immersed at 150 °F (65.5 °C) for 500 continuous hours. For moisture absorption comparison purposes, graphite/epoxy specimens were environmentally conditioned along with the hybrid specimens. Initially, it was planned to condition the test specimens at room temperature. However, the very slow moisture absorption rate of these materials (estimated to be 0.011% per day) made an elevation in temperature necessary to accelerate the moisture preconditioning phase of the investigation. The sensitivity of the polyethylene fiber to elevated temperatures has been noted [2]. Personal communication with Dr. Don Adams [15], a researcher in the area of polyethylene composites, resulted in the selection of 150 °F for the temperature of the ocean water solution. His work concluded that operation of the material at temperature sufficiently lower than 250 °F (121 °C) has some but not a dramatic effect on the mechanical behavior of the polyethylene fiber.

## Fatigue Testing

Fatigue testing was performed on an MTS servo-controlled, closed loop testing machine operating in the load-controlled mode. All testing performed was tension-tension axial fatigue with a constant load ratio (R) of 0.1. The fatigue test frequency was initially set at 10 Hz; however, preliminary hybrid test specimens exhibited hysteretic heating resulting in a specimen surface temperature increase in excess of 20 °F (11 °C) above ambient. A decrease in the cyclic frequency to 5 Hz reduced this temperature increase to 15 °F (8.3 °C). Air-cooling one side of the specimen by means of a fan reduced the hysteretic heating to an acceptable 5 °F (2.8 °C). All other tests were completed using this cooling arrangement.

Using the measured ultimate tensile strength values, a series of preliminary fatigue tests were conducted to establish proper stress levels for subsequent tests. The aim was to determine the maximum cyclic stress level which produced fatigue lifetimes on the order of one hundred thousand cycles. The results of these tests provided a working maximum stress of 55% of the UTS. This maximum stress amplitude was used in all subsequent tests.

Continuous stiffness monitoring was an integral part of damage development assessment. Strain for the fatigue tests was measured using a 2 in. (50 mm) gage length extensometer mounted to the center of the specimen so as to straddle the impact damaged area. Load was obtained from the MTS load cell.

Two types of fatigue test were done. In the "one shot" series of tests the specimen initial impact damage was assessed prior to the specimen being cyclicly loaded to a point thought to be near failure. At this point the specimen was removed from the testing machine and the damaged reassessed. The remaining series of tests were "stop and go" tests wherein the specimen was removed at periodic points in its fatigue lifetime.

Stiffness was monitored both statically and dynamically. By recording load and strain on a two channel plotter, the static elastic modulus could be calculated. To obtain

such a curve, the specimen was subjected to a half cycle loading at a frequency of .1 Hz. Static stiffness curves for each specimen were acquired initially and periodically throughout the tests.

The dynamic stiffness was monitored by a data acquisition system shown schematically in Figure 8. This system consisted of a Tektronix 4051 computer coupled with a Transera Analog/Digital converter and Tektronix 4631 hardcopier. The data acquisition system was initialized with specimen dimensions, calibration factors, and cyclic frequency for each test. The system acquired 1000 load and strain voltage data pairs over a 30 second time span, and calculated the dynamic stiffness approximately every 355 cycles using a least squares linear regression algorithm. The system displayed continuously the present stiffness,  $E$ , as well as the initial stiffness,  $E_0$ , number of cycles, and normalized stiffness reduction,  $(E_0 - E)/E_0$ . The system was also able to supply a plot of the normalized stiffness,  $E/E_0$ , as a function of cycles. The aim was to be able to stop the fatigue testing at predetermined values of stiffness reduction. Initial fatigue life tests indicated that for each material this curve was characteristic. A full discussion of the implications of the stiffness versus cycle curve (hereafter referred to as the stiffness reduction curve) is essential to the understanding of damage growth and necessarily will be deferred to a subsequent section. However, because the procedure followed in the fatigue portion of the experiment is based on this behavior, it is worthwhile at this point to briefly describe the regions of the stiffness reduction curve. Prior work in the area of graphite composite laminates revealed that pure graphite composites exhibit a dynamic stiffness reduction curve with three distinct regions: a region of rapid initial stiffness reduction, an intermediate region wherein the stiffness is linear with respect to cycles, and region III, a region of rapid stiffness reduction ending in specimen fracture [4].

The introduction of the polyethylene into such a laminate alters this phenomenon dramatically. The characteristic stiffness reduction curve for the hybrid composite material exhibits only two regions: a region of initial rapid stiffness reduction, and a linear

region in which the stiffness approached a horizontal asymptote. Figure 9 shows the general shape of the stiffness reduction curve for this material.

For the stop and go series of tests, the specimen was cyclicly loaded until the stiffness reduction curve reached the apparent end of Region I. The specimen was then unloaded, and reloaded for 1/2 cycle to obtain a static stiffness measurement. Two of the four stop and go test specimens of each type were edge replicated. During edge replication the specimen was loaded to its mean cyclic load†, and a replica was made of the edge over a length of 1 in. (25 mm) near the specimen center. (The edge replication technique as well as other damage evaluation methods are described in detail in a subsequent section of this report.) Following replication, the specimen was removed from the testing machine and prepared for X-ray radiography by the introduction of an X-ray opaque enhancing agent. Following X-ray radiography and a low temperature heating cycle (1 hour at 100° F (38° C)) to drive off the enhancing agent liquid carrier, the specimen was returned to the testing machine for further fatigue testing. During the examination phase, the extensometer mounting tabs were not removed. This stop and go process typically continued until the specimen failed in fatigue. Because Region II of the stiffness versus cycle curve is horizontal (i. e. very little stiffness reduction), dynamic stiffness monitoring proved an invalid stopping point selection technique. With the exception of the first point, subsequent stopping intervals were typically selected to be 50000 cycles.

The stop and go series of tests had the advantage that it provided clear evidence of damage progression in a given specimen. The method had the disadvantage that there were largely uncontrollable extraneous factors involved such as specimen realignment, extensometer calibration and alignment, introduction of a foreign substance (acetone for replication and enhancing agent for radiography) which made quantitative interpretation of the total stiffness reduction and damage development difficult.

---

† mean cyclic load = |max load during fatigue - min load during fatigue|/2

For this reason the complementary series of one shot tests were conducted. In these tests the specimen initial static stiffness was measured and initial radiography was performed. The specimen was then cyclicly loaded to a point thought to be near failure. Cyclic loading was terminated, a static stiffness calculation was made, and the specimen was removed for evaluation. The specimen was not tested in fatigue again.

## **Nondestructive Evaluation**

### **1. Edge Replication**

Replication is a technique by which surface topography is duplicated and made permanent in another medium. Jamison [4] made extensive use of this NDE technique in his investigation of conventional graphite composites. In order to use the technique effectively for composite materials, the specimen edges must be polished. The polishing procedure followed is similar to that used in metallography. Successively finer grades of abrasives are used to produce a desirable level of surface smoothness. For this study, the abrasives were wetted 240, 320, 400, and 600 grit silicon carbide paper, followed by 0.005 mm alumina powder on a wetted felt cloth. Each specimen edge was polished approximately 100 strokes at each polishing stage, reversing the polishing direction every 25 strokes. Edges were polished on all specimens whether or not they would be used in edge replication. This procedure was to prevent the addition of other factors in the the investigation (i. e. polished versus unpolished behavior).

To produce a replica of a polished edge, a piece of cellulose acetate tape, 10 mils in thickness, is affixed to the specimen edge with adhesive tape. A small amount of acetone is injected between the tape and specimen, and the tape is pressed quickly and lightly against the specimen edge. The acetate tape is allowed to harden for approximately one minute, and upon removal retains a permanent, high fidelity replica of the edge topography. The replica is then mounted and labelled on a glass plate for storage. Examination of the replica can be accomplished several ways. One means is by use of a microfiche

reader. When the glass plate containing the replica is inserted into the reader, magnifications on the order of 24X and 48X are provided. These are more than sufficient to distinguish the details of ply cracking and delamination which occur at the edge.

## 2. X-ray Radiography

X-ray radiography is perhaps the most widely used nondestructive evaluation technique aside from visual inspection for material characterization. In principle it provides images of material internal structure by the selective absorption and transmission of X-ray radiation. Variations in X-ray absorption in a composite material can result from the presence of voids, cracks, delaminations, inclusions, or manufacturing flaws. However, variations in X-ray radiation absorptivity among the classes of defects and damage mentioned are often slight and difficult to resolve in the X-ray image. As a result, it has become common practice in the radiography of composite materials to introduce an enhancing agent to these defects. In this study, zinc iodide was used as the enhancing agent. It is both diffusive and opaque to X-rays and consequently appears distinctly in X-ray images.

The zinc iodide solution consisted of 60 g of zinc iodide, 10 ml of water, 10 ml of isopropyl alcohol and 10 ml of Kodak "Photo-Flo 200" as a wetting agent. Although this solution is quite diffusive into the damage regions of the dry composite materials, the high moisture content of the environmentally conditioned specimens interfered considerably with the introduction of the enhancing agent [4].

It was therefore necessary to investigate a more effective way of enhancing agent infiltration than the present method of soaking. It was found that by subjecting one side of the specimen to a vacuum and the other side to the zinc iodide solution, the solution was pulled into the delaminations and other defects in the area of impact. Modeling clay was used to form a cup on one side of the specimen in which the zinc iodide solution was placed. This arrangement also included a plexiglass plate equipped with a recessed O-ring enclosing a 3/4 in. (19 mm) hole. The specimen was placed on the plate such that the

hole was directly beneath the impact area of the specimen. The vacuum pump tubing was equipped with a rubber attachment which, when placed on the underside of the plexiglass, created a suction which in turn subjected the specimen to a vacuum. Figure 10 shows this arrangement.

Radiographs of the specimens were made immediately after zinc iodide treatment using a Balteau Electric Company Model BS160 X-ray unit. The nominal film-to-source distance was 26 in. (660 mm). By a series of preliminary trials, the optimum operating voltage for the laminates used was found to be 5kV. The film used was Kodak Industrex R-type, single emulsion and high resolution. The exposure time was 5.0 minutes. A light table was sufficient for preliminary examination. Prints were made from the negatives for final result analysis.

### **3. Ultrasonic C-scan**

An attempt was made to use ultrasonic C-scanning techniques to map the damage growth in the test specimens. In principle, C-scanning provides internal damage locations by the transmission and attenuation of ultrasonic sound. The sound is transmitted to the specimen from the source via a carrier (usually water). The sound travels through the solid giving a reflection off the front face as well as the back face. Voids, delaminations, cracks, and other damage modes attenuate ultrasonic sound and thus present a premature reflection. C-scan digitally stores this information, and is capable of creating a clear picture of internal damage.

Ultrasonic scanning was available at the University of Delaware, and permission was obtained for its use. The first specimen scanned was conventional graphite. The specimen had been impacted and the scan was able to substantially map the damage. An impacted hybrid specimen was also scanned. The test specimen was scanned at frequencies ranging from 2.5 to 20 MHz. At any of the frequencies, no back face reflection was achieved. It was the opinion of the machine's trained operator that no more than two plies had been penetrated. It is conjectured that the porosity of the polyethylene fibers

attenuated the sound, thus making this NDE technique unsuitable for damage growth mapping for the hybrid material.

## Discussion of Results

### *Static Testing*

Static testing on both graphite and hybrid specimens confirmed that strength had indeed been sacrificed to obtain potential toughness. The average graphite UTS for the six specimens tested was  $107.85 \pm 4.52$  Ksi ( $743 \pm 31.1$  MPa). The six hybrid test specimens yielded an UTS of  $40.93 \pm 2.53$  Ksi ( $282 \pm 17.4$  MPa). However, volume and weight measurements of these specimens before static testing yielded densities of 0.056 (1.553) and 0.023 (0.638) pounds per cubic inch (g/(cm<sup>3</sup>)) respectively. Two types of fatigue tests were done. The first series of tests were "one shot". The graphite specific strength was  $1.915 \times 10^6$  in. (48938 m) as compared to a specific strength of  $1.78 \times 10^6$  in. (45212 m) for the hybrid material. Consequently, the specific strengths of the two materials do not differ dramatically. For comparison, the specific strength of A93004 aluminum is approximately 255000 in. (6477 m) and that of 1045 high-strength steel is 908000 in. (23063 m). Hence, although the specific strength of the hybrid composite was lower than that of graphite/epoxy, it still exceeded the values for most competitive metals.

Static testing also provided information concerning the modulus of elasticity of both materials. The average graphite/epoxy modulus was found to be  $8.79 \pm 13$  Msi ( $60.6 \pm 0.90$  GPa). However, in calculating the elastic modulus for the hybrid material, it was noted that the stress-strain curve was nonlinear. The nonlinearity of this curve gave evidence that this material was subject to creep. In order to obtain the modulus in the elastic region, it was necessary to perform a linear regression on a selection of points from each curve. This calculation resulted in an average hybrid elastic modulus of  $4.34 \pm 18$  Msi ( $29.9 \pm 1.24$  GPa). Hence, the specific modulus for graphite and hybrid material were  $157 \times 10^6$  in. ( $3.99 \times 10^6$  m) and  $188 \times 10^6$  in. ( $4.78 \times 10^6$  m) respectively. In this instance the hybrid material was specifically stiffer than the graphite material.

### *Initial Impact Damage*

Composite material damage exists in several forms, including fiber breakage, delamination, interface damage, and voids. It was found that initial impact created several modes of damage. For each impacted specimen, the damage was characterized by a small dimple (approximately 0.5 in. (13 mm) in diameter) on the impact side and a ring of cracks on the opposite side. Inside this 1.0 in. (25 mm) ring, cracks in the shape of a crucifix were also visible. Because the downward deflection of the specimen was constrained by the pipe, the upper plies were crushed as characterized by the ring of cracks. The resulting damage was fiber fracture and fiber-matrix interface damage. The crucifix on the underside of the specimen implied the formation of both a longitudinal crack and a transverse crack in the bottom plies.

Graphite specimens were also impacted, and the initial damage assessed and compared. Radiographs of both graphite and hybrid composite specimens were taken immediately after impact and showed that initial graphite damage was much more distinct and localized. The initial longitudinal and transverse cracks on the underside of the graphite specimens were more evident in the radiographs. The damage modes were not seen in the hybrid specimens until the specimens were well into their fatigue life. It was expected that the fiber breakage in the graphite specimens was much more severe due primarily to the lack of polyethylene fibers which absorbed impact energy in the hybrid specimens. The graphite specimens were not subjected to fatigue.

### *Moisture Absorption*

The moisture absorption percentage for each specimen used in fatigue testing is presented in Table 2. After soaking in the synthetic ocean water, the hybrid material absorbed  $2.91 \pm 0.47\%$  by weight. Similarly conditioned graphite specimens were also evaluated. These specimens averaged  $1.47 \pm .33\%$  moisture addition. This finding is consistent with previously published literature in this area 8,10,11.

Moisture absorption is accomplished primarily by the matrix. Very little moisture absorption can be attributed to the individual fibers. In this study both hybrid and graphite test panels were fabricated similarly with the same matrix. How then can the discrepancy in the moisture absorption between these two materials be explained? The answer to this question lies with the consideration of the polyethylene fiber interface. The fiber-matrix interface is characterized by small voids which, when the specimen is subjected to moisture, provide room for the water. These wet specimens also experienced an average 1.66% increase in thickness due to swelling.

#### *Fatigue Behavior*

During fatigue testing, the nonlinear behavior of the hybrid composite was again evident. Throughout these tests a digital storage oscilloscope was used to continuously monitor the loading and unloading curves for the specimen being tested. It was found that for this material the curves form a hysteresis loop as shown in Figures 11-12. The hysteresis loop describes the strain response of the material during repeated or reversed loading, and is associated with the anelastic effects, plastic deformations, and with the formation and growth of cracks [13]. The figures present hysteresis loops for both dry and wet material. The left loop of each figure was acquired during the first thousand cycles. The right curve loop was acquired near failure. These curves introduce four results to be discussed:

- 1) The concept of increased strain energy which is represented by the opening characteristic of the loops
- 2) decreasing curve slope
- 3) The bimodal characteristics of the second curve
- 4) The nonlinearity of the curves and implied viscoelastic behavior

The energy that a material absorbs as the result of deformation under load is called strain energy. By definition, the total work done on a body by loading up to some value

of deformation is:

$$W = \int_0^e P de$$

where            W = work done  
                  P = load  
                  e = deformation

The area under the loading curves thus represents the total energy transferred to the specimen. The elastic strain energy, that energy that can be recovered as the loading is released, is represented by the area under the unloading curve. Therefore, the area of the loop depicts the strain energy absorbed by the specimen. The energy is dissipated either by hysteretic heating as discussed previously, or by damage growth. As noted by the increase in the area of the hysteresis loop, the strain energy absorbed for this material increased as life was expended by fatigue. Two possibilities exist as to by what means this additional energy was dissipated. One possibility is that hysteretic heating increased. While no significant increase in temperature was noted, this possibility can not be discounted since the surface temperature of the specimen was not monitored during this portion of the test. Another possible source of energy dissipation is internal friction and damage growth.

The curves shown in Figure 11-12 also possess varied slopes each of which represent the dynamic stiffness modulus at that point in the test. Because this stiffness modulus was used as a damage analog, it was monitored continuously by the data acquisition system described earlier. The system used the method of least squares to calculate this modulus every 71 seconds. Continuous monitoring by the system yielded stiffness reduction curves for both dry and wet specimens in Figures 13-14. It was found that the absolute value of the dynamic stiffness was slightly greater than the static stiffness which was plotted on the two channel plotter. Although the absolute stiffness measurements varied, the static and dynamic stiffness reductions varied only slightly. It was then feasible to use the dynamic stiffness reduction as a damage analog to control the fatigue tests.

Figures 11-12 are consistent with Figures 13-14 which present typical stiffness reduc-

tion curves for the hybrid dry and wet specimens. These figures show that the overall stiffness reduction for wet specimens were on average higher than the dry specimens. This greater stiffness reduction is attributed to the moisture plasticizing the resin allowing it to flow from the fibers. The overall stiffness then is lower because it no longer has any contribution from the matrix.

The bimodal characteristic of the righthand curves of Figures 11-12 can be related to the damage mode and growth in the area of interest. During the initial cycles, the fiber-matrix interface was relatively undamaged, and the fiber weave was constrained by the matrix. As the specimen is subjected to more cycles, the fiber-matrix interface becomes damaged causing the release of the fiber weave. Allowing the weave to "unkink" gives the hysteresis loop its bimodal shape with two apparent stiffnesses. The first stiffness modulus was geometry-related, resulting from the unkinking of the weave. Once the weave reached maximum deformation, the mechanical behavior of the individual fibers dominated resulting in the second slope.

The hybrid material exhibited viscoelastic (time dependent) characteristics. This behavior can be explained by examining the load-sharing mechanisms between the fibers. When a group of similar fibers are subjected to a load, each shares equally load equally. If the fibers are dissimilar and exhibit dissimilar mechanical behavior, each type of fiber responds to the load differently. This varying response can alter the load division. So it is with this material. When subjected to a uniform, constant load, the material equally divided the load initially. However, because the polyethylene fibers were more compliant than the adjacent graphite fibers, they stretched to alleviate the load. This stretching gradually "dumps" the load carried by the polyethylene fibers into the graphite fibers. They, in turn, deform under the increased load resulting in a time-dependent deformation for the material.

### *Damage Growth*

X-ray radiography proved a very effective method of evaluating and tracking the damage through the laminates. Figure 15 shows X-rays of a dry specimen at various stops in its lifetime. Figure 16 presents X-rays for a wet specimen. Each set of X-rays represent a typical stop-and-go test for the specimens. The static stiffness reduction (SSR) of each test is also included. The reproductions show how the damage propagates through the material as it is subjected to fatigue. The increase in the impact damage area for the wet specimens was much greater than that of dry specimens. The increase for all specimens can be obtained from Figures 17-18. These figures plot the damage area ratio as a function of the static stiffness reduction. This nondimensionalized area ratio is the damage area per area between the tabs. The line represents the best fit of these data points. The most obvious result from the plots is clear: the damage area increases with SSR. However, slopes of these best fit lines raises a possible result which leads only to speculation. Why does an incremental damage area result in a larger incremental static stiffness reduction for the wet specimens when compared to the dry incremental stiffness reduction for the same incremental damage area? It is believed that added moisture in the composite material along the fiber-matrix interface which has been identified as weak, creates a condition whereby the resin becomes debonded from the fibers. Under undamaged conditions, both resin and fiber contribute to the overall stiffness of the material. The debonding of the resin from the fibers results in a stiffness whereby the resin contributes nothing. Consequently, the stiffness reduction for wet specimens is higher. It is important to note that without time-consuming sectioning, this hypothesis cannot be confirmed.

Edge replication also contributed information concerning damage growth. Prints of typical edge replicas are included in Figure 19. Also included is the SSR at the point the replica was made. Information gained from these prints describe the damage modes experienced by the specimens at the edge. As shown the material experienced increasing number of cracks as stiffness reduction and cycles increase. Although the edges were pol-

ished, cyclic loading deteriorated the topography of the edges rapidly. Additionally, the cutting process also caused delaminations at the edges by pulling out fibers running along the cut. These delaminations are seen as white vertical stripes on the prints. The cracks initiated at these delaminations and followed the fiber-matrix interface. It was also found that the number of cracks per unit length for the wet specimens exceeded that of the dry.

#### *Material Failure*

While the specimens were undergoing the fatigue testing, loud reports were heard as individual graphite fibers failed. Additionally, one could even see the deformation of the polyethylene in the surface plies.

The initial transverse crack on the back face became more pronounced as fatigue continued. This crack increased in size moving toward one edge. However, ultimate failure resulted more often from a crack unnoticed initially. This crack began either at the top or bottom of the initial ring of cracks. Tests concluded that most specimens which failed in fatigue, failed at a 45 degree angle as the specimen shown in Figure 20. Failure resulted in total fracture of graphite fibers. The polyethylene fibers did not break, rather they stretched and ripped.

#### **Conclusions**

Several conclusions were achieved by this investigation:

- 1) Specific strength of the hybrid material is slightly lower than that of conventional carbon/epoxy composite materials, but higher than most metals.
- 2) When subjected to the same impact energy, conventional graphite material experiences initial damage which is more localized and severe than that of the hybrid material.
- 3) The hybrid material exhibits viscoelastic behavior. This behavior results in increased strain energy absorbed by the specimen during fatigue loading. This strain energy is dissipated by hysteretic heating and damage growth.

- 4) More moisture is absorbed by the hybrid material when subjected to the high moisture environment due to the poor polyethylene fiber-matrix interface.
- 5) The stiffness reduction for environmentally conditioned hybrid material is more significant than that of hybrid dry material. One possibility exists that the resin in the wet material no longer contributes to the material's overall stiffness.
- 6) Wet hybrid material damage growth is more evident than dry material damage growth due to accelerated debonding of the epoxy resin.

The hybrid composite material can possibly contribute significantly to the reduction of damage growth in composite material structural applications, yet the servicability of this material cannot be determined until more work is done. The behavior of the material first must be compared to that of currently-used composite materials subjected to the same fabrication process and experimental program. Although a comparison was made of the initial crack tolerance of both hybrid and graphite material, and it was found that the hybrid material excelled in this area, no graphite material was subjected to fatigue due to machine constraints, and thus no damage growth information is available.

More research must be done to improve the fiber-matrix interface of the polyethylene. This may be done by either improving the resin matrix or improving the surface adhesion of the individual fiber by surface treatment. It is recognized that surface treatment may not be utilized in the weave application due to the severe degradation of the fiber surface by the weaving process.

## NEAT RESIN PROPERTIES

SPECIFIC GRAVITY	1.336 g/cc
T <sub>g</sub> DRY	250 °F
EQUILIBRIUM MOISTURE ABSORPTION	9.4%
LINEAR COEFFICIENT OF THERMAL EXPANSION	2.93 x 10 <sup>-5</sup> in/in/°F
TENSILE STRENGTH	11.6 ksi
TENSILE MODULUS	0.47 msi
TENSILE STRAIN	5.2%
FRACTURE TOUGHNESS, K <sub>1c</sub>	1.50 ksi $\sqrt{\text{in}}$
	1.37 MPa $\sqrt{\text{m}}$
STRAIN ENERGY RELEASE RATE, G <sub>1c</sub>	4.18 lb/in
	0.73 KJ/m
GEL TIME @ 250 °F	4-10 min.

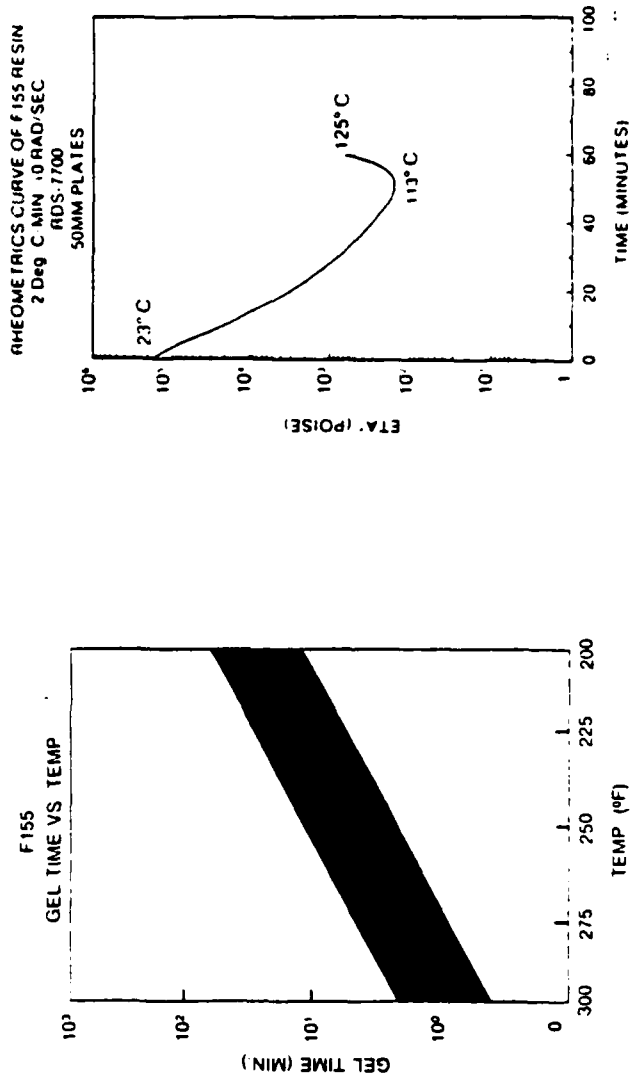
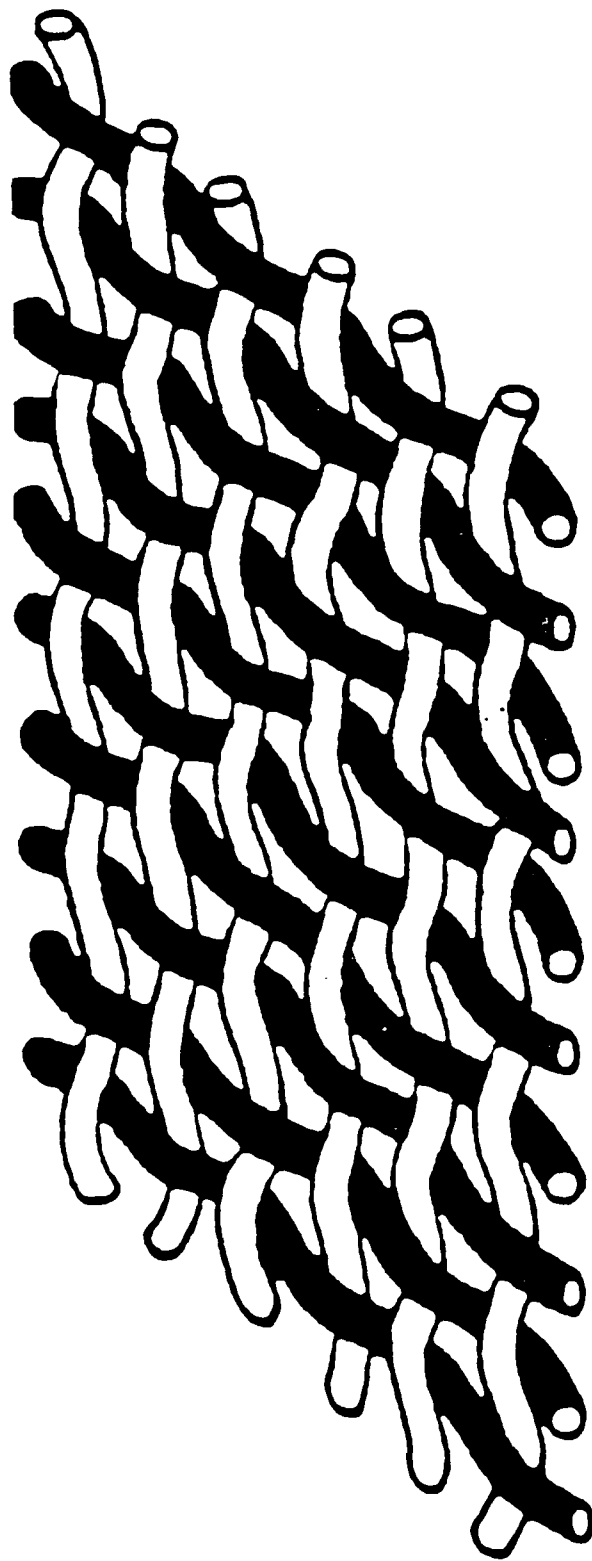


FIGURE 1

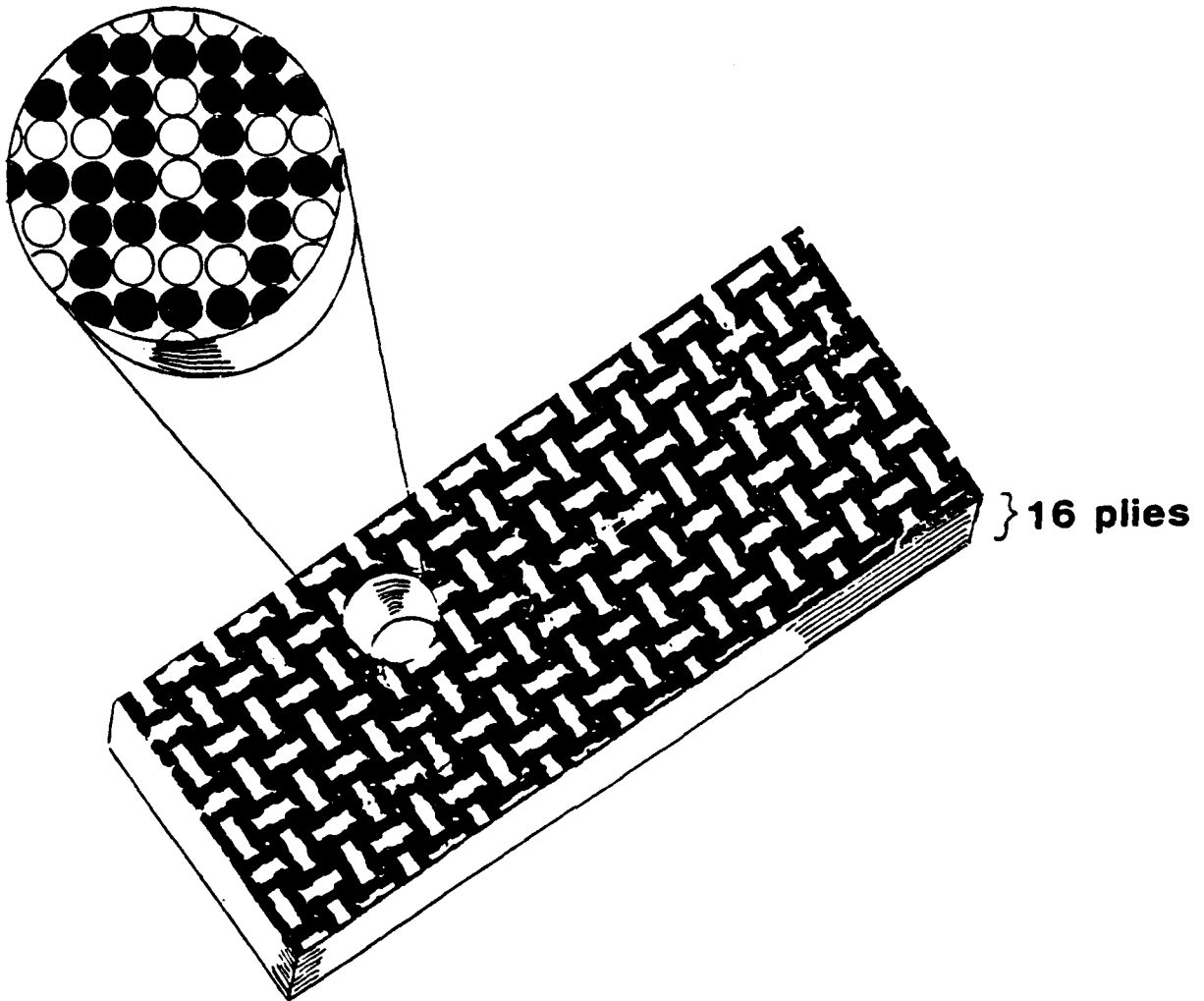
# 2-D WOVEN FABRICS



PLAIN

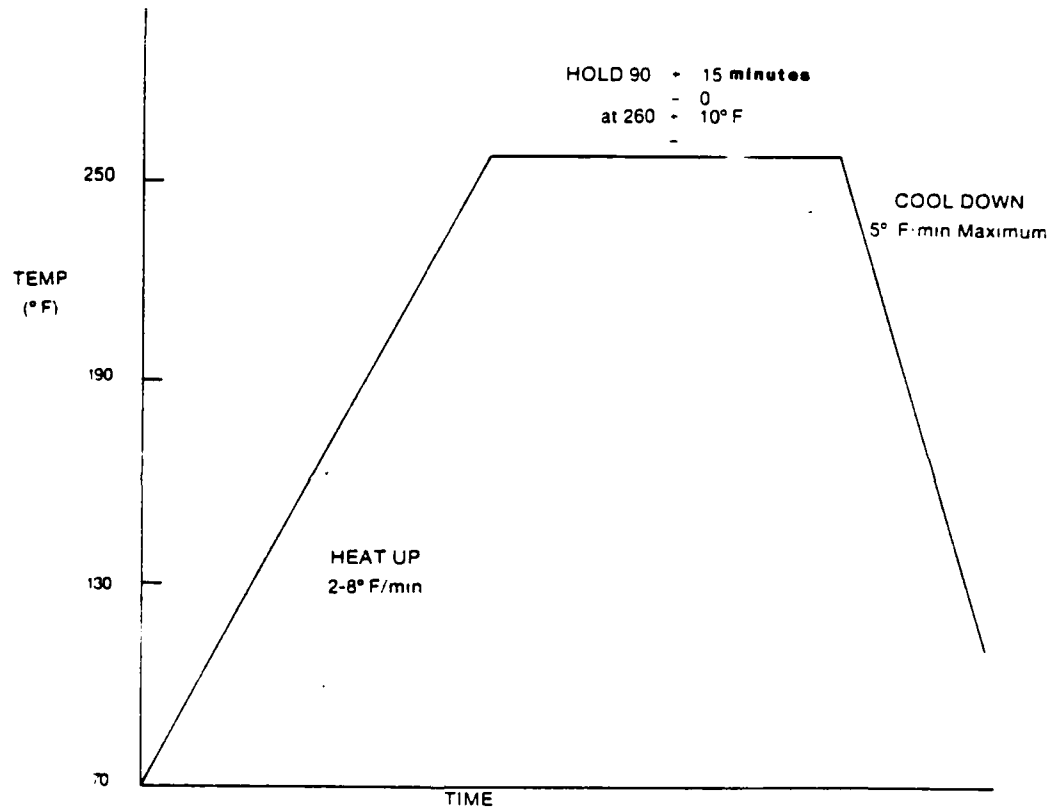
FIGURE 2

**FIGURE 3**



**Hybrid Weave Pattern**

**FIGURE 4**  
CURE CYCLE



**CURE PROCEDURE.**

- A Apply vacuum of 22 in. Hg minimum
- B Apply 85 - 15 - 0 PSIG pressure for laminates.
- C Apply 45 - 15 - 0 PSIG pressure for sandwich \*
- D Vent vacuum bag to atmosphere when pressure reaches 20 PSI
- E During cool down when the part temperature falls below 140° F. pressure can be relieved and the test panel removed from the autoclave and debagged.

\*Typical for HRH 10-1.8-3.0 honeycomb

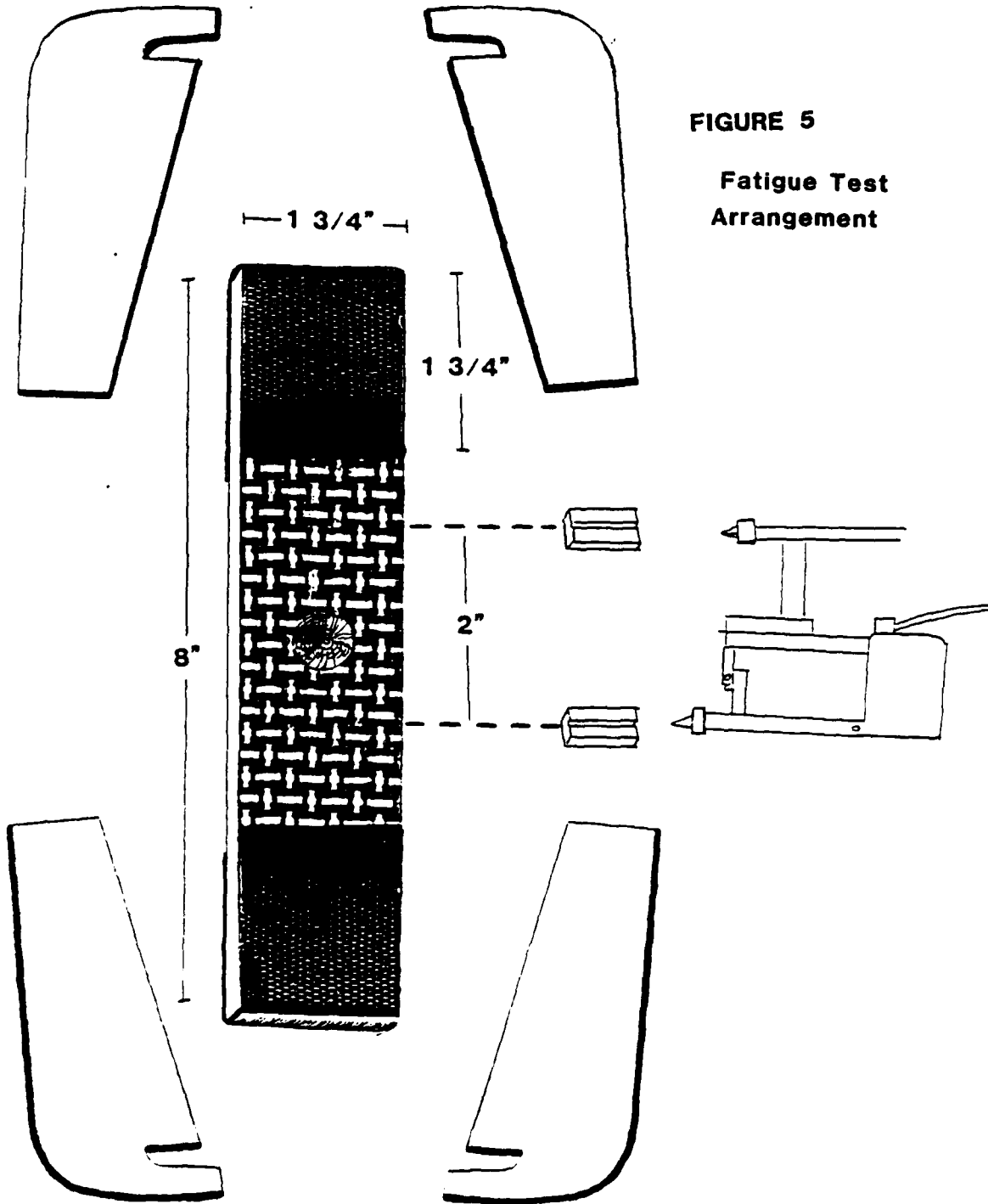
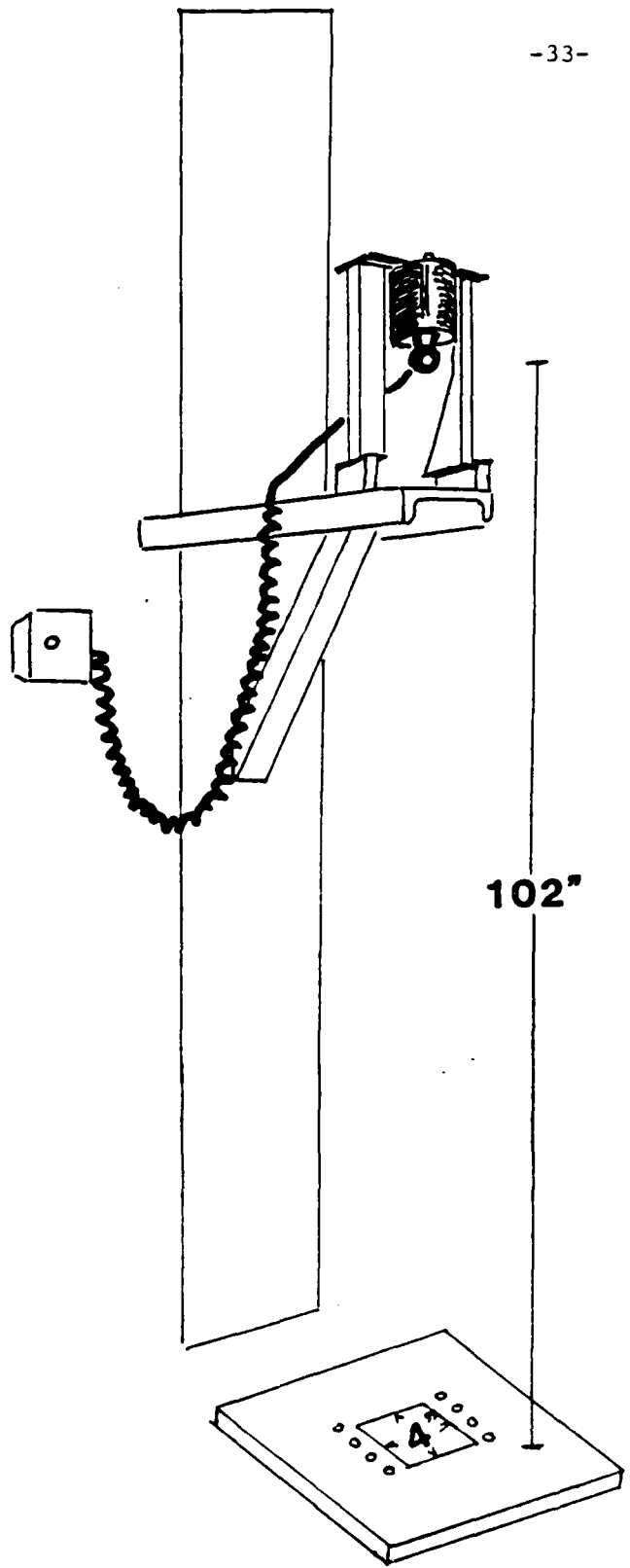


FIGURE 5

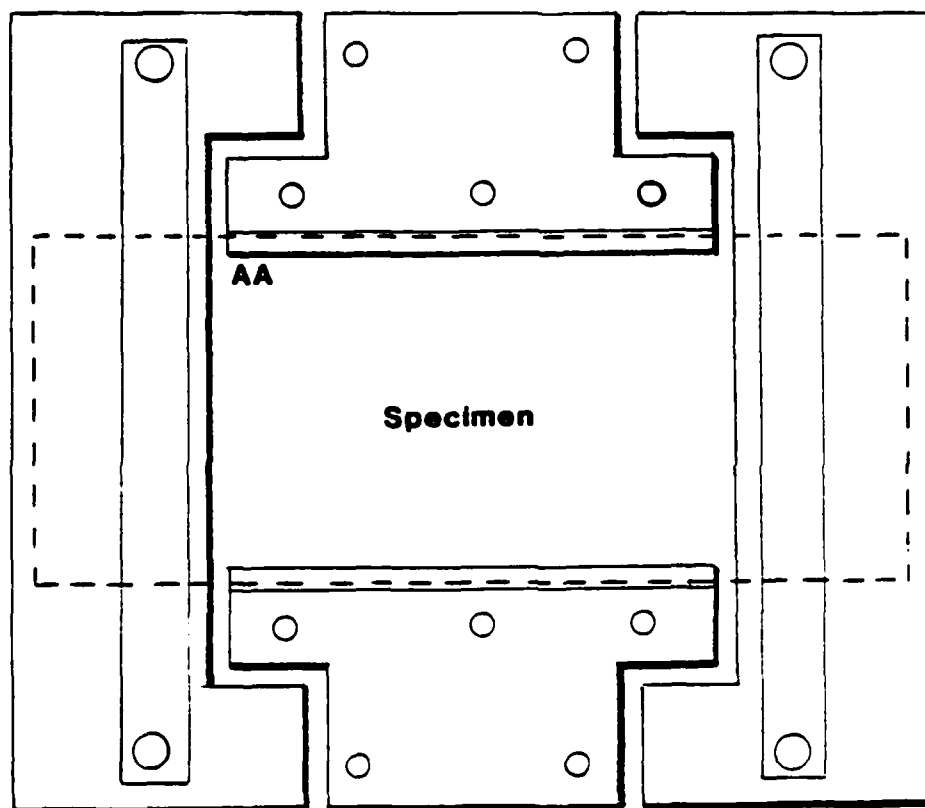
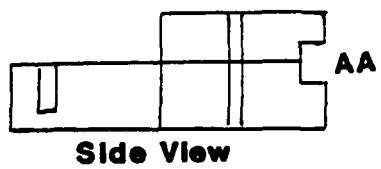
Fatigue Test  
Arrangement



102"

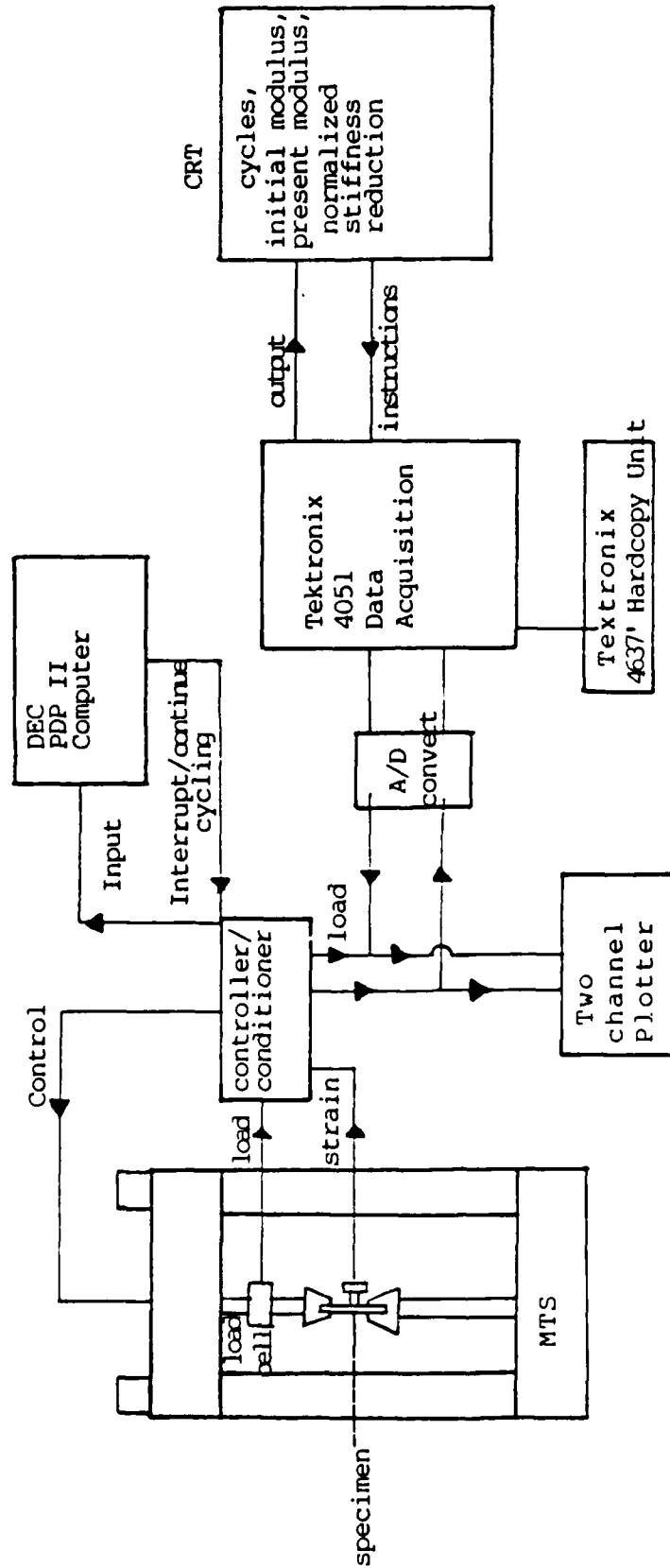
Drop Tower

FIGURE 6



**Specimen Constraint Fixture**

**FIGURE 7**



Data acquisition and control during fatigue testing.

FIGURE 8

# Typical Stiffness Reduction Curve

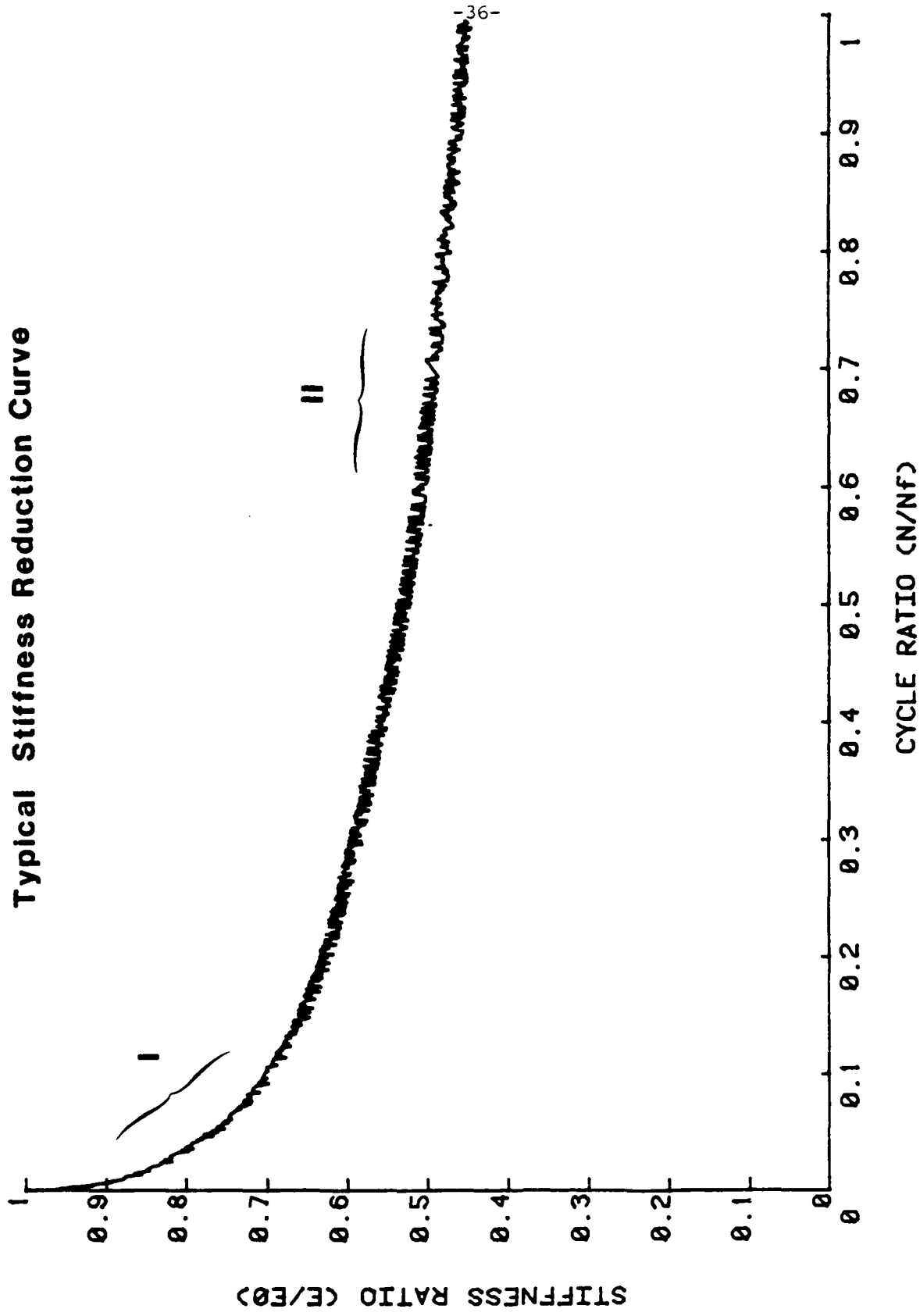
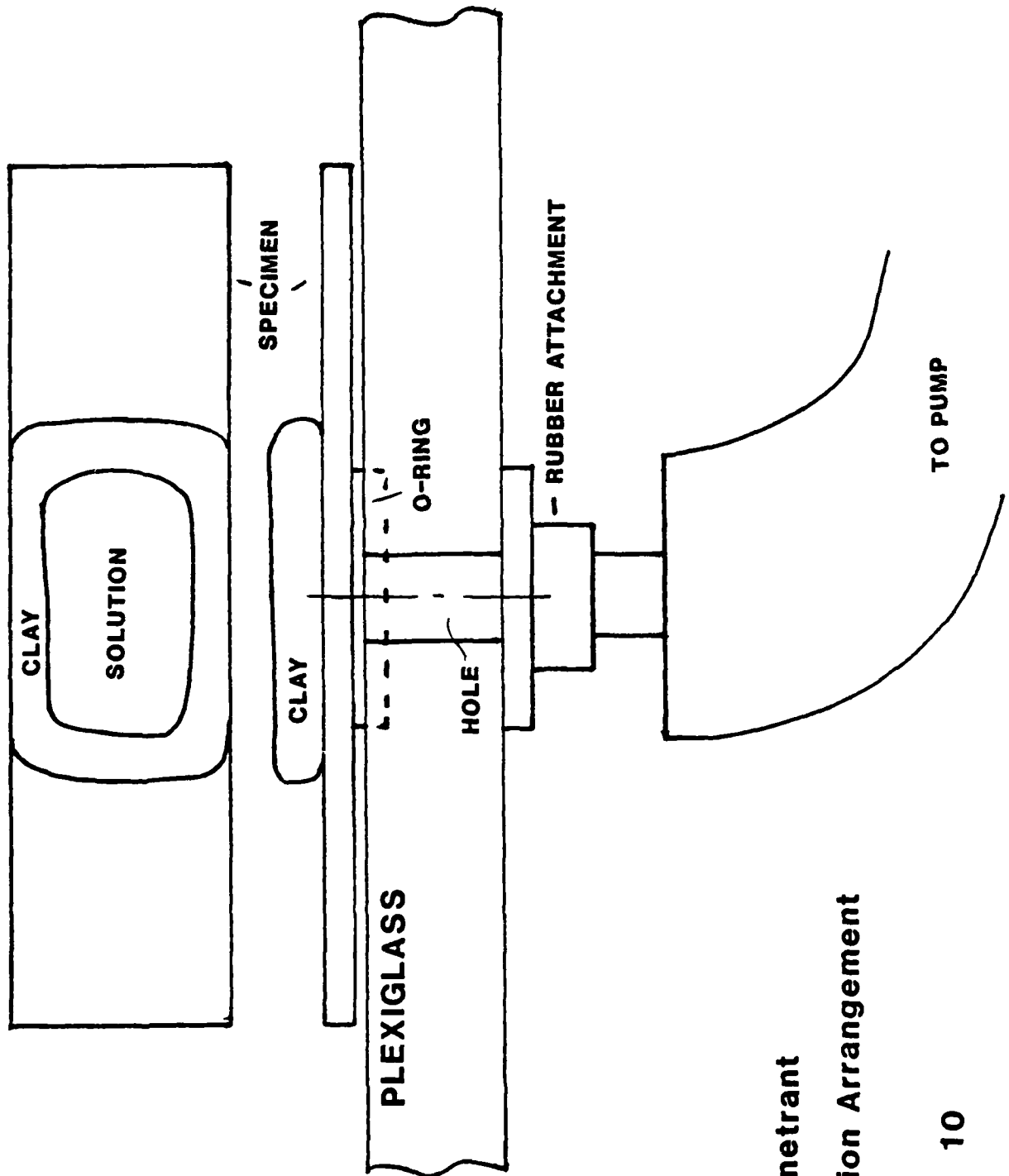


FIGURE 9





**Dye Penetrant  
Infiltration Arrangement**

**FIGURE 10**

# HYSTERESIS CURVES DRY SPECIMEN

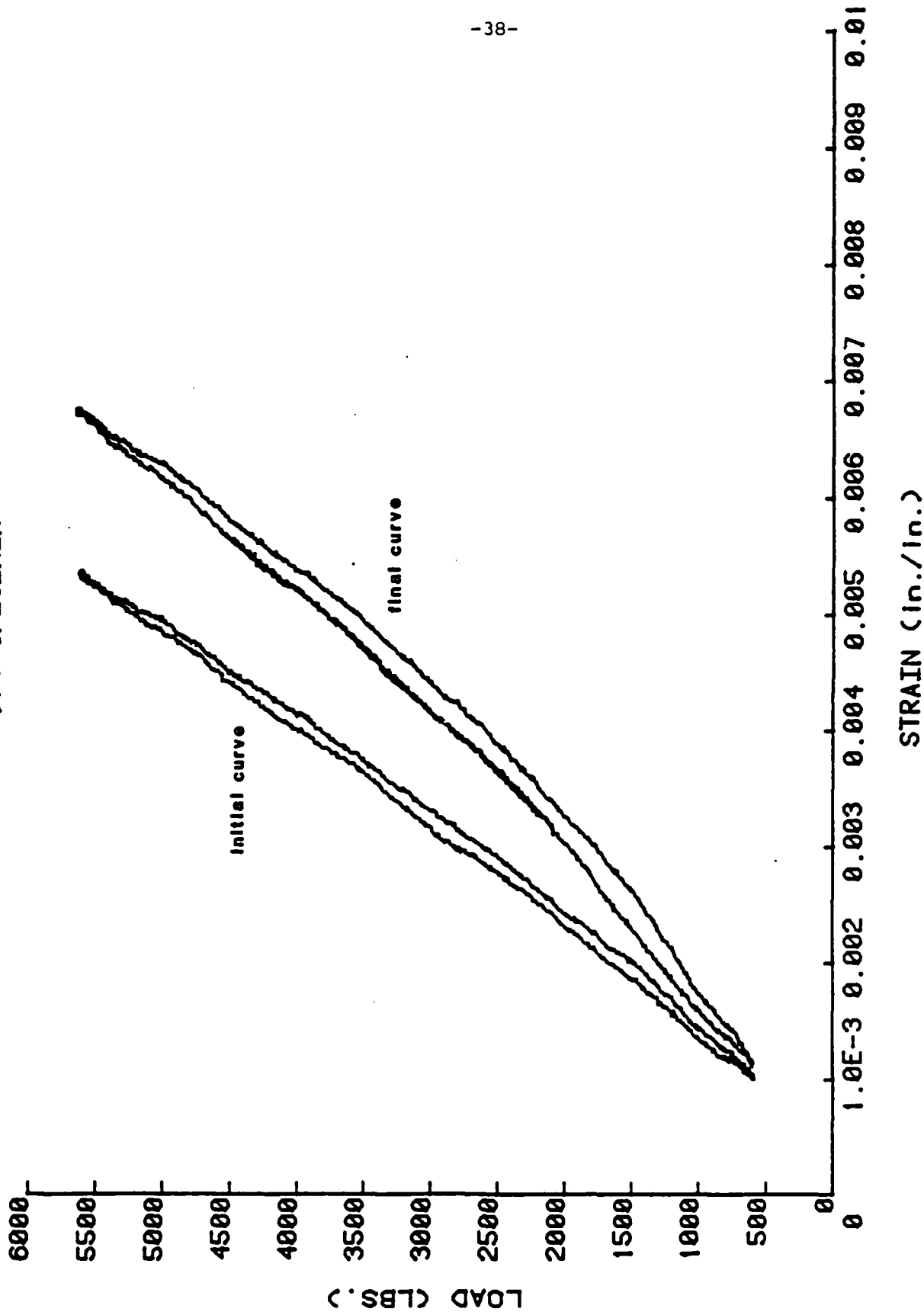
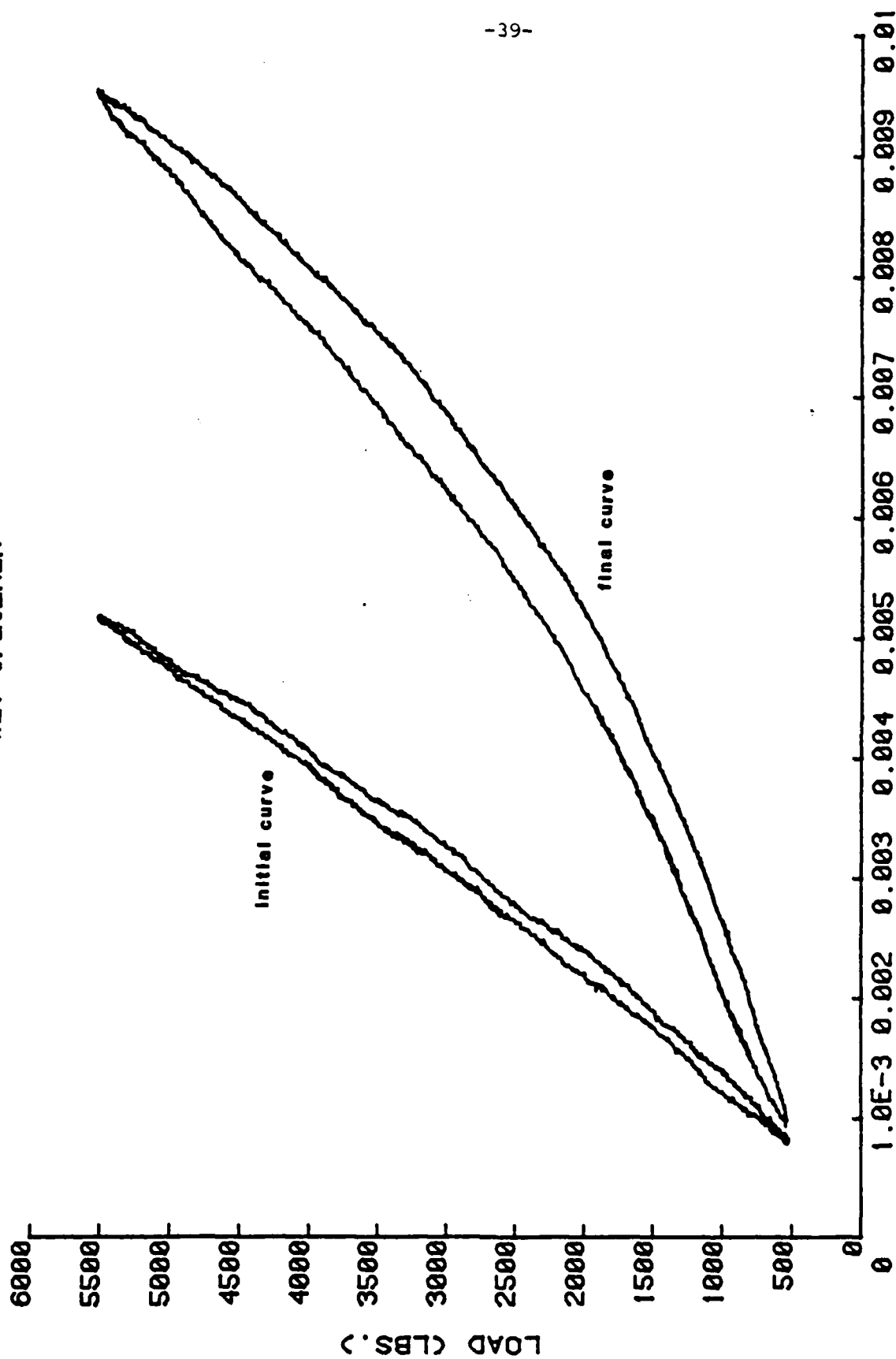


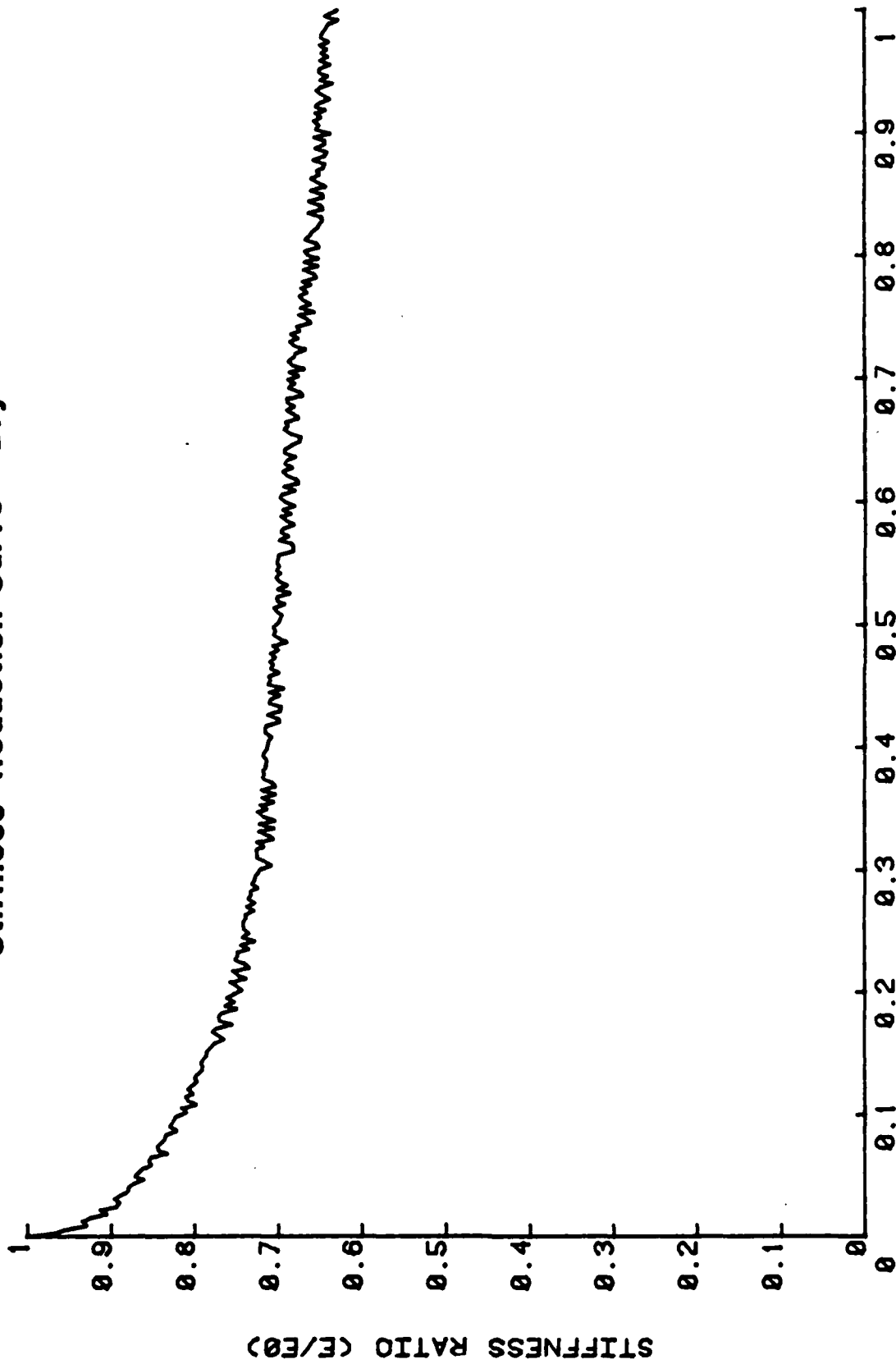
FIGURE 11

HYSTERESIS CURVES  
WET SPECIMEN



STRAIN (in./in.)  
FIGURE 12

# Stiffness Reduction Curve - Dry



CYCLE RATIO (N/Nf)

FIGURE 13

### Stiffness Reduction Curve - Wet

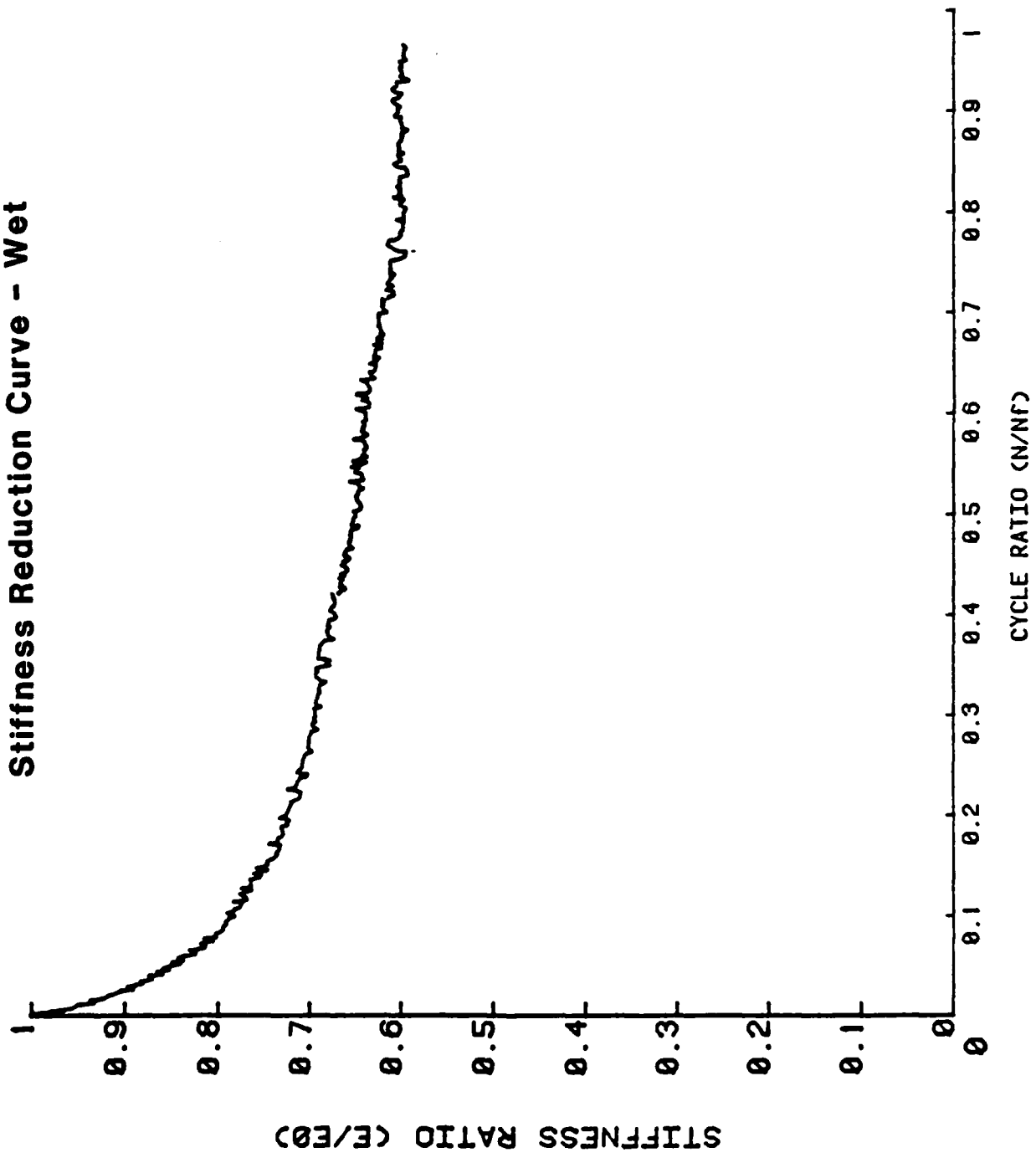


FIGURE 14

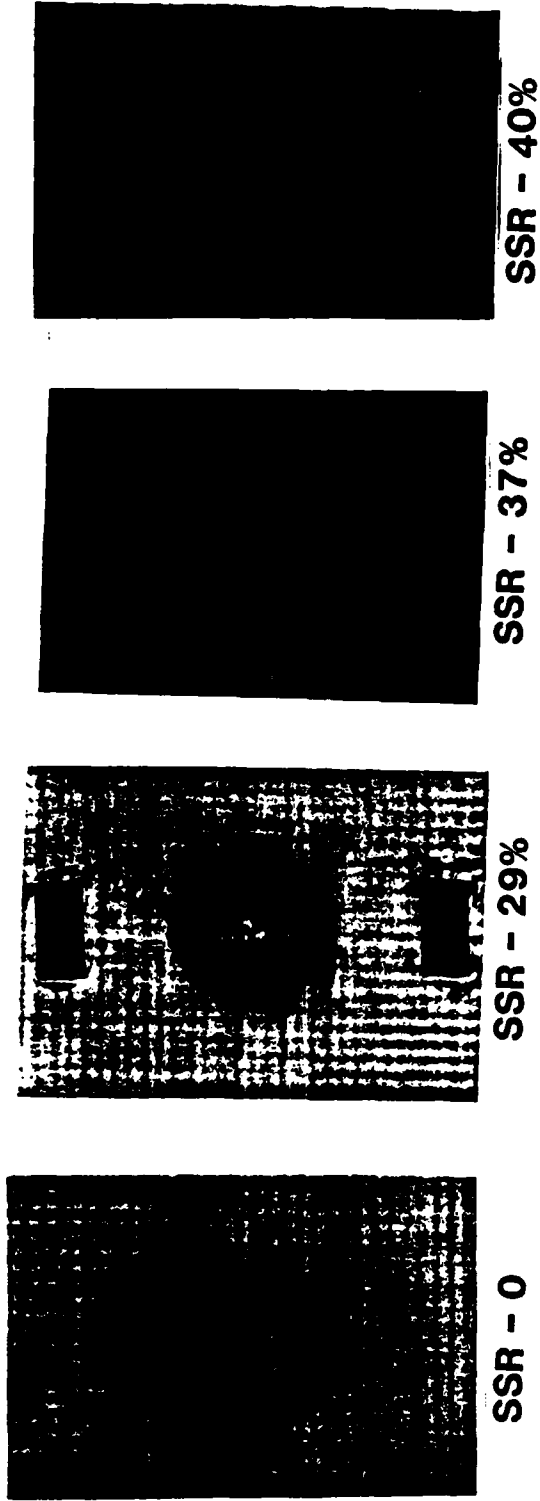
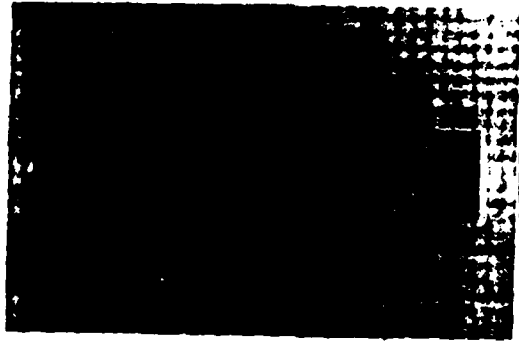


FIGURE 15 Damage Growth - Dry Material

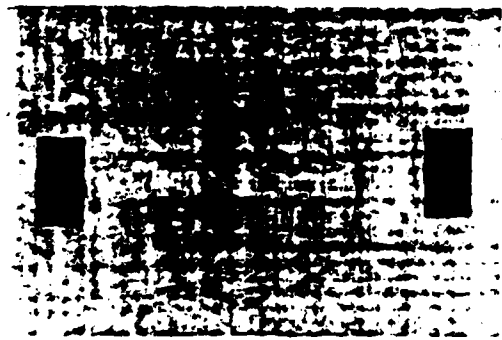




SSR - 64%



SSR - 62%



SSR - 56%



SSR - 0

FIGURE 16 Damage Growth - Wet Material

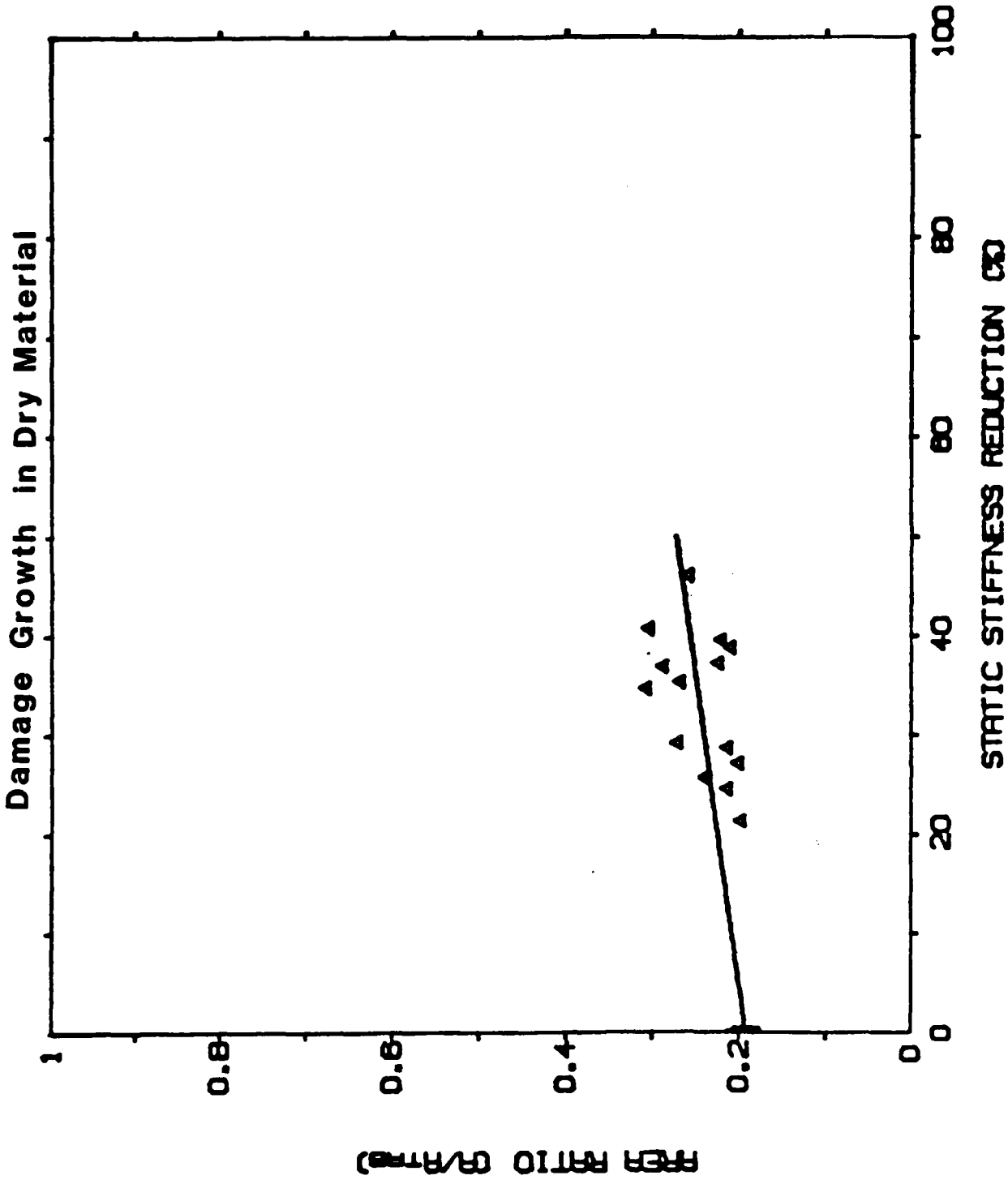


FIGURE 17

STATIC STIFFNESS REDUCTION (%)

Damage Growth in Dry Material

RRR RATIO (RATED)

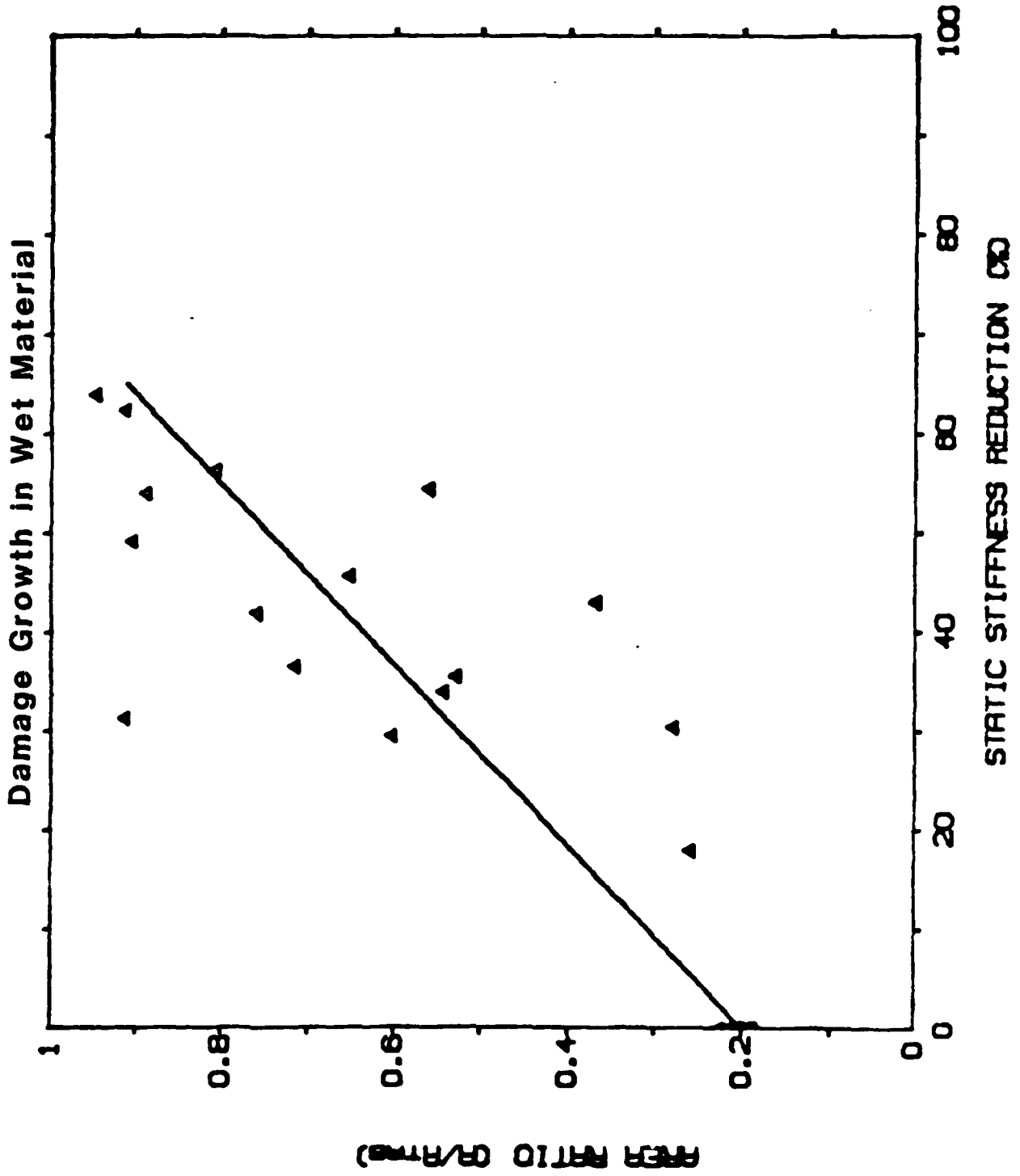


FIGURE 18



SSR- 54%



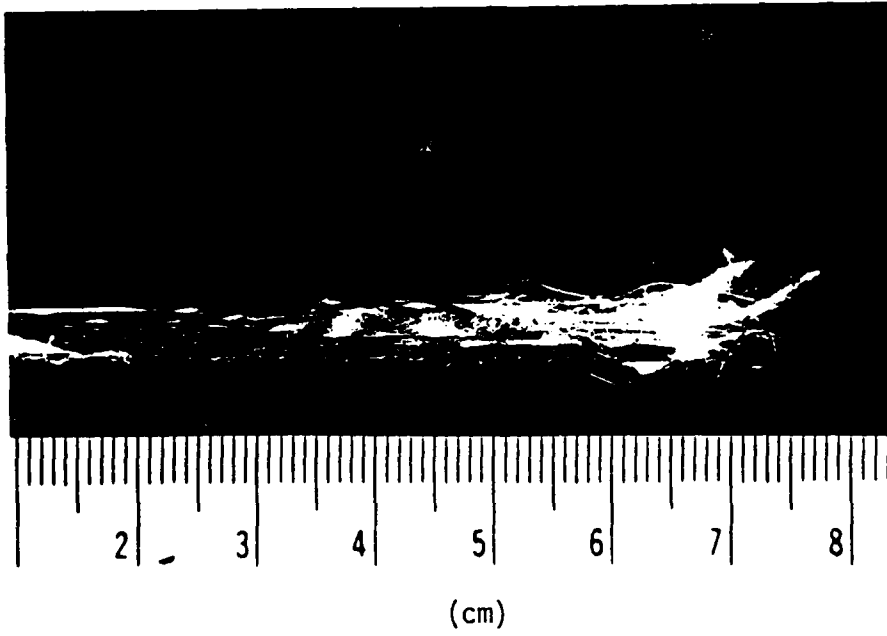
SSR- 49%



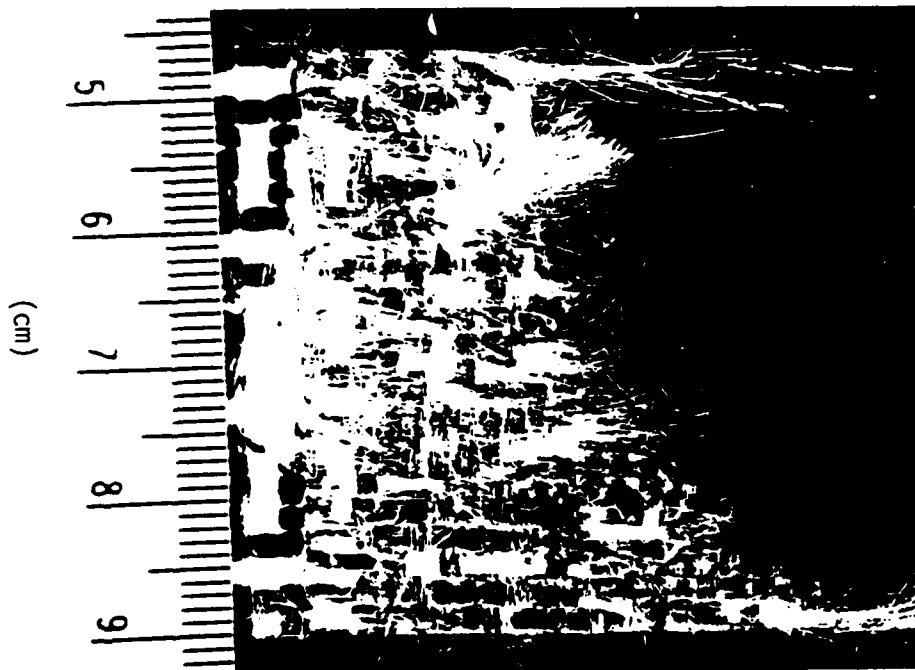
SSR- 0

FIGURE 19: Edge Replicas





**Edge**



**Surface**  
**Fatigue Failure**  
**FIGURE 20**

Static Testing Summary		
Specimen No.	UTS Ksi	Elastic Modulus Msi
Graphite		
D-3	103.4	8.77
D-4	112.0	8.91
D-5	110.6	8.75
D-6	100.2	8.55
D-7	112.2	8.93
D-8	108.7	8.84
Average	107.85±4.52	8.79±0.13
Hybrid		
E-1	36.2	4.20
E-2	39.5	4.20
E-3	42.1	4.08
E-4	42.5	4.53
E-5	44.1	4.48
E-6	41.2	4.52
Average	40.93±2.53	4.34±0.18

Table 1

Hybrid Material Moisture Absorption Results			
Specimen Number	Original Weight (g)	Wet Weight (g)	Moisture Absorption (%)
H-2	46.10	47.63	3.21
H-3	45.83	47.39	3.29
H-4	45.83	47.33	3.17
H-6	45.80	47.10	2.76
H-9	46.35	47.83	3.09
M-5	44.88	46.10	2.65
M-6	44.78	46.08	2.82
M-7	45.11	46.24	2.44
M-8	45.12	46.38	2.72
Average	45.53±0.54	46.90±0.66	2.91±0.47

Table 2

**Acknowledgements**

The author wishes to acknowledge with gratitude the contributions of the following:

- Dr. Russell D. Jamison for his unending dedication and encouragement during this work.
- Allied Corporation for providing the test material.
- Dr. J. Joyce for the use of his testing equipment.
- The staff of the Advanced Composite Material Lab, DTNSRDC, for use of their equipment and advice.
- The technicians associated with Technical Support Division for their unending patience and help.
- The Mechanical Engineering Department staff for its yearlong support.

## References

1. Chamis, C. C., and Lark, R. F., "Hybrid Composites - State-of-the-Art Review: Analysis, Design, Application, and Fabrication," NASA TM 73545, March 1977
2. Fuss, J. L., Engineer, Composites Lab, NARF, Personal Communication, Cherry Point, NC, 21 February 1986.
3. Jamison, R. D., Schulte, K., Reifsnider, K. L., and Stinchcomb, W. W., "Characterization and Analysis of Damage Mechanisms in Tension-Tension Fatigue Graphite/Epoxy Laminates," *Effects of Defects in Composite Materials*, ASTM STP 876, 1984.
4. Jamison, R. D., *Advanced Fatigue Damage in Graphite Epoxy Laminates*. Ph. D. Dissertation, Virginia Polytechnic Institute and State University, 1982.
5. Jones, Robert M., *Mechanics of Composite Materials*, Washington D. C.: Scripta Book Company, 1975.
6. Adams, D. F., Zimmerman, R. S., and Chang, Heh-won, "Properties of a Polymer-matrix Composite Incorporating Allied A-900 Fiber," *Proceedings of the 30th National SAMPE Symposium*, Anaheim, California, March 1985.
7. Eaton, G. A., *Ballistic Damage of Graphite Epoxy Plates*, Dissertation, Naval Postgraduate School, 1977.
8. Altman, J. M., and Olsen, W. G., "Qualification of Low-cost Composite Secondary Structures," Air Force Flight Dynamics Laboratory Technical Report-77-129, December 1977.
9. Ramkumar, R. L., "Environmental Effects on Composite Damage Criticality." Technical Report NADC-79067-60, January 1982.
10. Blikstad, M., Sjoblom, P. W., and Johannesson, R. T., "Longterm Moisture Absorption in Graphite Epoxy Angle-ply Laminates," *Journal of Composite Materials*. January 1984, pp. 32-46.
11. Lifshitz, J. M., "Strain Rate, Temperature, and Humidity Influences on Strength and Moduli of a Graphite Epoxy Composite," *Composite Technology Review*, Vol. 4, No. 1, Spring 1982, pp. 14-19.
12. Hancox, N. L., "Environmental Response of Hybrid Composites." *Journal of Material Science*, Vol. 19, No. 6, June 1984, pp. 1969-1979.
13. Carswell, W. S., *Hysteresis and Environmental Effects in Fatigue of Composite Materials*, International Symposium 'Composite Materials and Engineering', University of Delaware, September 24-28, 1984.
14. Boll, D. J., Bascom, W. D., and Motiee, B. *Moisture Absorption by Structural Epoxy-Matrix Carbon-Fiber Composites*, International Symposium 'Composite Materials and Engineering', University of Delaware, September 24-28, 1984.
15. *Annual Book of ASTM Standards 1985*. Specifications for Substitute Ocean Water. D114-75 (1980).
16. Adams, R. F., Professor, University of Wyoming, Laramie, Wyoming, Personal Communication, Petersburg, Virginia, October 1985.

## Appendix A

### Preparation of Substitute Ocean Water

#### *Stock Solution No. 1*

The following salts were dissolved in water and diluted to 7.0 liters:

MgCl 6H O	3889.0 g
CaCl (anhydrous)	405.6 g
SrCl 6H O	14.8 gi

#### *Stock Solution No. 2*

The following salts were dissolved in water and diluted to 7.0 liters:

KCl	486.2 g
NaHCO	140.7 g
KBr	70.4 g
H BO	19.0 g
NaF	2.1 g

245.34 grams of sodium chloride (NaCl) and 40.94 grams of anhydrous sodium sulfate (Na SO ) was dissolved in 8 to 9 liters of water. 200 mL of Stock Solution No. 1 and 100 mL of Stock Solution No. 2 were added slowly. The solution was then diluted to 10.0 liters. The pH was adjusted to 8.2 by adding 0.1 N sodium hydroxide (NaOH) solution.